



**HAL**  
open science

# Carbon-Carbon Bond Forming Reactions in Diazines via Transition Metal-Catalyzed C-H Bond Activation

Rafael Gramage-Doria, Christian Bruneau

► **To cite this version:**

Rafael Gramage-Doria, Christian Bruneau. Carbon-Carbon Bond Forming Reactions in Diazines via Transition Metal-Catalyzed C-H Bond Activation. *Synthesis: Journal of Synthetic Organic Chemistry*, 2023, 10.1055/a-2134-0307 . hal-04167894

**HAL Id: hal-04167894**

**<https://univ-rennes.hal.science/hal-04167894>**

Submitted on 3 Aug 2023

**HAL** is a multi-disciplinary open access archive for the deposit and dissemination of scientific research documents, whether they are published or not. The documents may come from teaching and research institutions in France or abroad, or from public or private research centers.

L'archive ouverte pluridisciplinaire **HAL**, est destinée au dépôt et à la diffusion de documents scientifiques de niveau recherche, publiés ou non, émanant des établissements d'enseignement et de recherche français ou étrangers, des laboratoires publics ou privés.

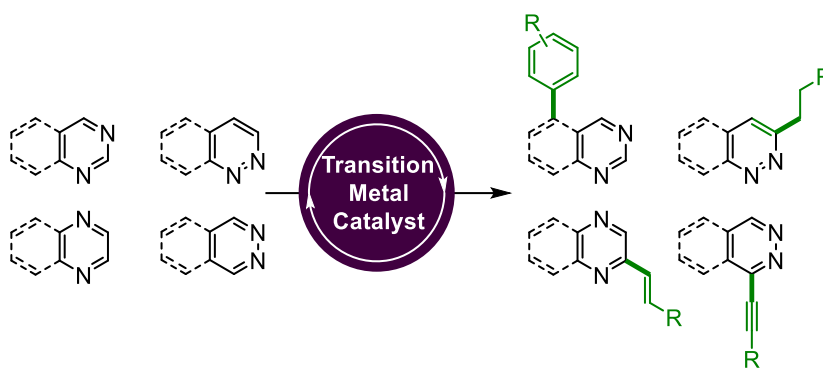
# Carbon-Carbon Bond Forming Reactions in Diazines via Transition Metal-Catalyzed C-H Bond Activation

Rafael Gramage-Doria<sup>a\*</sup>  
Christian Bruneau<sup>a</sup>

<sup>a</sup> Univ Rennes, ISCR UMR 6226, F-35000 Rennes, France

rafael.gramage-doria@univ-rennes1.fr

[Click here to insert a dedication.](#)



Received:  
Accepted:  
Published online:  
DOI:

**Abstract** An overview of the key achievements concerning carbon-carbon bond-forming process with diazines under transition metal-catalyzed C-H activation is presented. Focus is devoted to those examples in which the C-H functionalization takes place in the diazine or the benzodiazine core because of its relevance in material sciences and as active pharmaceutical ingredients. These metal-catalyzed protocols take benefit from the biased reactivity of the C-H bonds targeted or from the presence of a rationally-designed directing group at proximity of the C-H bond to be functionalized. As such, innovative alkylations, alkenylations, alkynylations, arylations and carboxylations are accomplished within such skeletons in a step- and atom-economy fashion.

1. Introduction
2. Transition metal-catalyzed C-H alkylation of diazines
3. Transition metal catalyzed C-H alkynylation of diazines
4. Transition metal-catalyzed C-H alkenylation of diazines
5. Transition metal catalyzed C-H arylation of diazines
6. Transition metal-catalyzed C-H carboxylation of diazines
7. Conclusion

**Key words** diazines, C-H activation, arylation, alkenylation, alkylation, metal catalyst

## 1 Introduction

Aromatic heterocycles containing more than one nitrogen atom are present in numerous molecules presenting a wide range of properties with applications in biological, optical and electronic fields. This is especially the case of diazine and benzodiazine derivatives featuring two nitrogen atoms in a six-membered aromatic ring (Figure 1).<sup>1,2</sup>

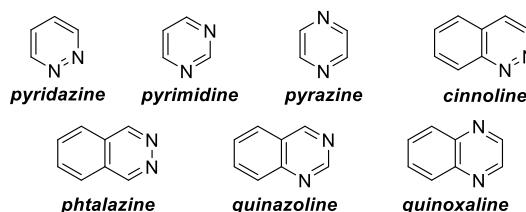


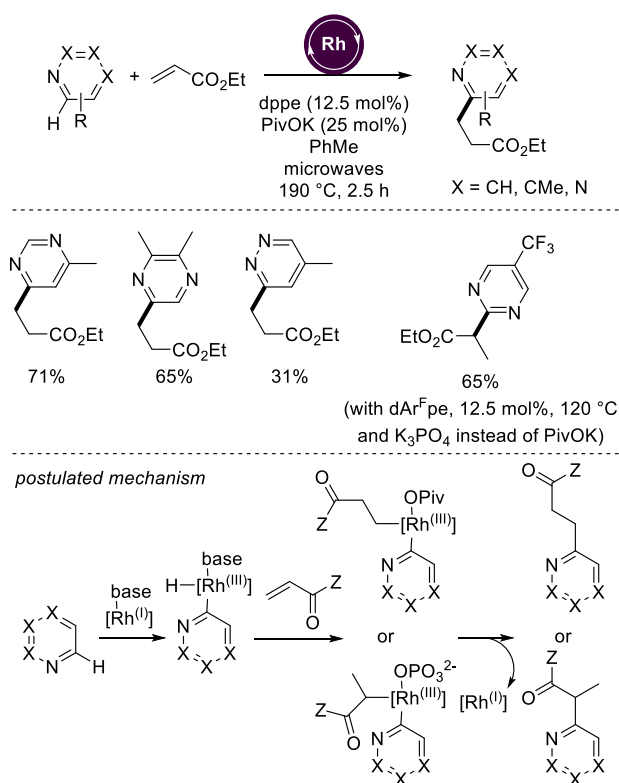
**Figure 1** Structural motifs of diazines and benzodiazines.

Functionalization of these primary substrate cores, which are known as electron poor heterocycles, have been achieved with various transition metal-free methods including nucleophilic aromatic substitution of hydrogen<sup>3</sup>, radical (Minisci-type) transformations,<sup>4</sup> and deprotonative metalation (lithiation, magnesiation, zincation) followed by quenching by an electrophile.<sup>5</sup> Transition metal-catalyzed cross coupling reactions between a diazine halide and an organometallic reagent (Suzuki-Miyaura, Stille, Negishi, Corriu-Kumada coupling), or a terminal alkyne (Sonogashira coupling), or an olefin (Heck coupling), have also been used for the formation of new carbon-carbon bonds in diazines,<sup>6</sup> but most of them generate harmful byproducts in stoichiometric amounts.

More straightforward and atom economic coupling methods based on direct C-H bond activation<sup>7a-7g</sup> have recently appeared making possible unprecedented functionalization of diazines.<sup>7h-7k</sup> In this review article we wish to focus on transition metal-catalyzed C-H bond functionalization of diazines and benzodiazines leading to the formation of new carbon-carbon bonds, namely alkylation, alkynylation, alkenylation, and arylation. Functional diazines such as diazinones, diazine-diones and diazine *N*-oxides presenting either modified reactivities or directing group properties have been considered beyond the scope of this contribution. All metal-catalyzed radical processes have not been included, and mechanistic considerations have been omitted.

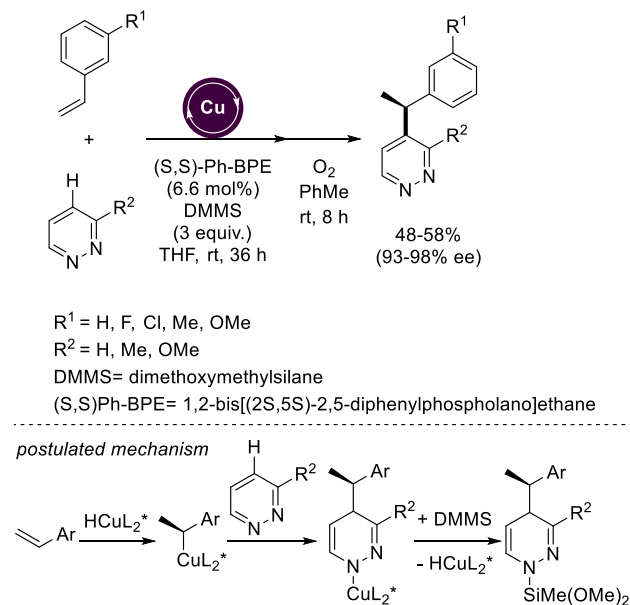
## 2 Transition metal-catalyzed C-H alkylation of diazines

The synthesis of alkylated diazines relies on two types of reactions: metal-catalyzed hydroarylation of alkenes and direct alkylation with alkyl halides. A catalytic system based on  $[\text{Rh}(\text{Cl}(\text{cod}))_2]$ , a diphosphine and a base catalyzed the *ortho*-selective alkylation of all kinds of diazines with ethyl acrylate and dimethyl acrylamide.<sup>8</sup> The regioselectivity of the alkylation was dictated by the migratory insertion of the electron-deficient double bond into a Rh-H bond generated by oxidative addition of the diazine to the metal centre. Linear alkylated products were obtained in the presence of potassium pivalate as a base whereas branched isomers were obtained when the more basic potassium phosphate was used (Scheme 1, top). The efficiency of the formation of branched products was improved by using the less basic 1,2-bis[3,5-bis(difluoromethylphenyl)phosphino]ethane (dArFpe) together with  $\text{K}_3\text{PO}_4$  as the base, as compared to 1,2-bis(diphenylphosphino)ethane (dppe), which gave good yields in the formation of linear products using PivOK as the base. The reaction mechanism involved a Rh(I)/Rh(III) catalytic cycle initiated by C-H activation in the diazine core followed by migratory insertion of the olefin with the regioselectivity controlled by the nature of the base (Scheme 2, bottom). Finally a reductive elimination affords the product while regenerating the active Rh(I) complex (Scheme 1, bottom). It is interesting to note that 3,4-dihydroquinazolines have been alkylated with various terminal alkenes at the  $\text{sp}^2\text{C}(2)$  position of the heterocycle with a catalyst based on  $[\text{RhCl}(\text{cyclooctene})]_2$  and tricyclohexylphosphine at 150 °C in THF.<sup>9</sup> In the presence of an excess of olefin and prolonged reaction time, aromatization of the 2-alkyl-3,4-dihydroquinazolines led to 2-alkylquinazoline *via* a cascade rhodium-catalyzed hydrogen transfer process. This aromatization could also be efficiently achieved by adding  $\text{MnO}_2$  as oxidant.



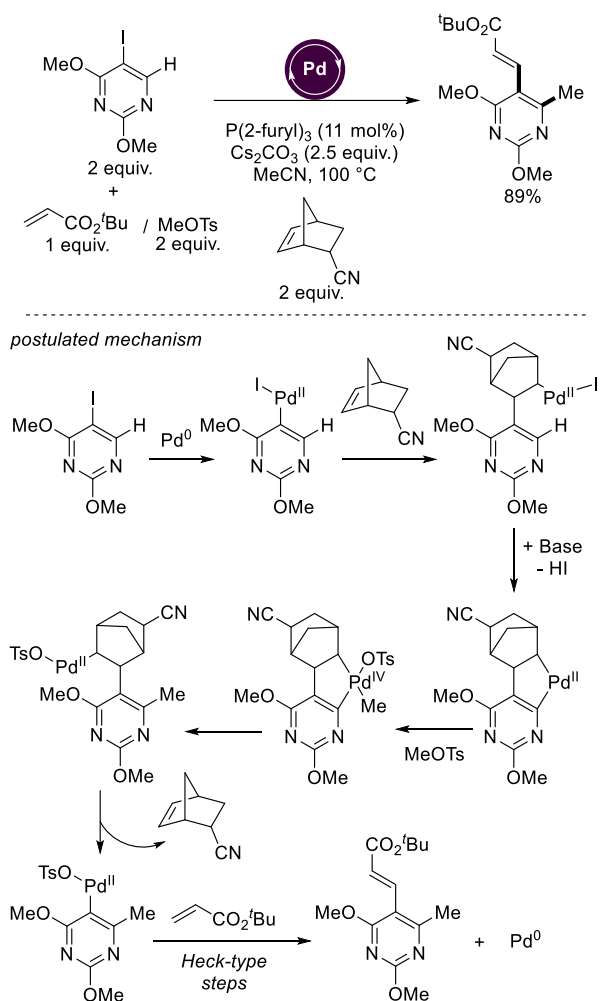
**Scheme 1** Rhodium-catalyzed alkylation of diazines with ethyl acrylate (top) and plausible reaction mechanism (bottom). Rh =  $[\text{Rh}(\text{Cl}(\text{cod}))_2]$  (10 mol%).

Enantioselective alkylation of pyridazines by styrenes has been successfully achieved with a chiral copper catalyst at room temperature (Scheme 2, top).<sup>10</sup> This reaction involved a dearomatization/reoxidation sequence starting with the formation of a copper hydride in the presence of dimethoxymethylsilane (DMMS) followed by regioselective insertion of the styrene double bond, which generated a chiral  $\alpha$ -methylbenzyl copper species with high enantioselectivity due to the presence of the optically pure (S,S)-Ph-BPE ligand (Scheme 2, bottom). This intermediate reacted with a copper-coordinated pyridazine to form a dearomatized *N*-cuprate leading to the formation of the optically active alkylated pyridazine after  $\sigma$ -bond metathesis with the silane. Further oxidation at room temperature gave the final optically active benzylated pyridazine.



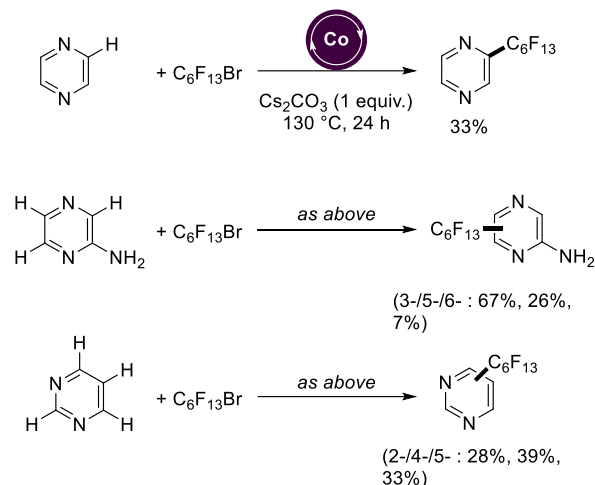
**Scheme 2** Copper-catalyzed enantioselective alkylation of pyridazines (top) and plausible reaction mechanism (bottom). Cu =  $\text{Cu}(\text{OAc})_2$  (6 mol%).

The palladium-catalyzed methylation/alkenylation of 2,4-dimethoxy-5-iodopyrimidine based on the Catellani strategy<sup>11</sup> has been proposed to achieve the Heck-type alkenylation with a *tert*-butyl acrylate and the alkylation with methyl tosylate<sup>12</sup> (Scheme 3, top). The benzylation of the analog 2,4-dimethoxy-5-bromopyrimidine was carried out in 57% yield under similar conditions with *p*-methoxybenzyl chloride as alkylating agent.<sup>13</sup> As depicted in Scheme 3 (bottom) the reaction starts with a Pd(0) species that undergo oxidative addition at the substrate followed by norbornene coordination and migratory insertion enabling methylation at the neighboring C-H bond prior activation of Pd(II) to Pd(IV) with the alkylating agent MeOTf. Reversible norbornene release followed by a palladium-catalyzed Heck process with the acrylate derivatives forms the final product and regeneration of the active Pd(0) species.



**Scheme 3** Palladium-catalyzed both alkylation/alkenylation based on Catellani strategy (top) and plausible reaction mechanism (bottom). Pd =  $\text{Pd}_2(\text{dba})_3$  (5 mol%).

The direct alkylation of diazines with unactivated alkyl halides is not very documented. Some modest results have been obtained using copper catalysis, for instance 35% yield of 5-substituted quinoxaline with  $\text{BrCF}_2\text{CO}_2\text{Et}$  as reagent, but the proposed mechanism was based on radical processes.<sup>14</sup> The monoperoalkylation of pyrazine and pyrimidine has been performed with  $\text{C}_6\text{F}_{13}\text{Br}$  as alkylating agent and stoichiometric amount of  $\text{Cs}_2\text{CO}_3$  at 130 °C with a heterogeneous nanocatalyst containing 10 mol% of cobalt that could be recycled several times (Scheme 4).<sup>15</sup> Mechanistic investigation ruled out the involvement of radicals.

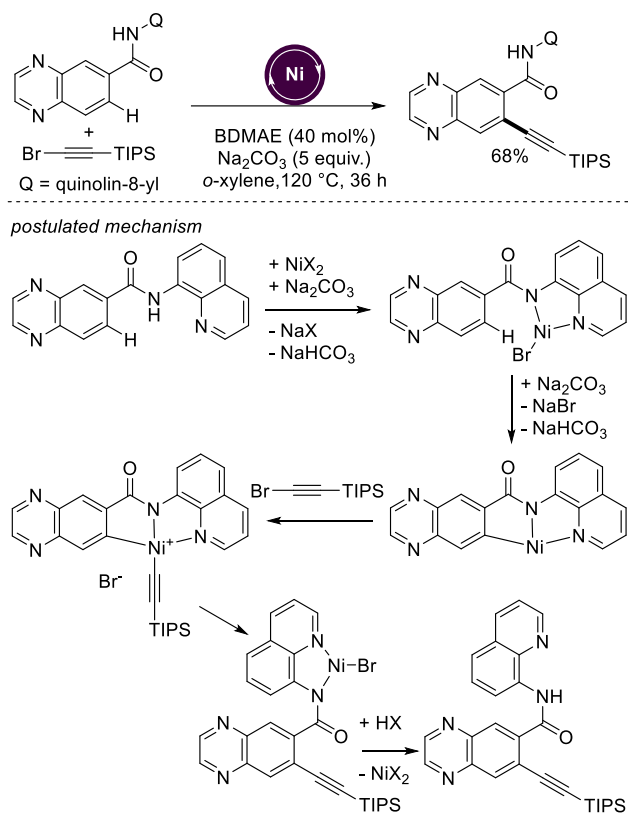


**Scheme 4** Perfluoroalkylation of diazines with a cobalt nanocatalyst. Co = cobalt nanocatalyst (10 mol%).

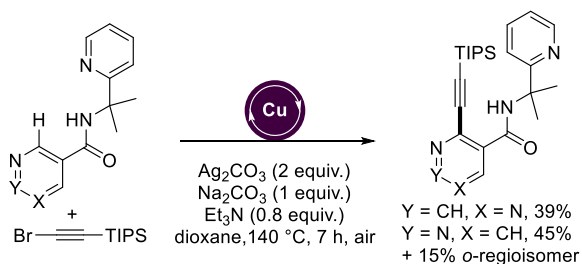
### 3 Transition metal catalyzed C-H alkylation of diazines

Transition metal-catalyzed alkylation has been performed with diazines featuring a pendant chelating functional group. With this strategy, regioselective directed C-H bond activation/alkylation could take place. Thus,  $\text{NiCl}_2$  in combination with bis(2-dimethylaminoethyl)ether (BDMAE) provided the regioselective *ortho*-alkylation by TIPS-protected bromoacetylene of the quinoxaline core substituted by a bidentate *N*-(quinolin-8-yl)amide (Scheme 5, top).<sup>16</sup> The chelating 2-(pyridin-2-yl)propan-2-ylamido group (PIP) linked to a monocyclic diazine triggered the *ortho*-directed C-H activation on the diazine structure *via* a concerted metalation deprotonation mechanism in the presence of a base (Scheme 5, bottom). The overall reaction mechanism follows oxidative addition of the bromoalkyne at Ni going from +2 to +4 formal oxidation state ending up with a reductive elimination and regeneration of the active nickel(II) species (Scheme 5, bottom). With copper catalysts known to also activate the C-H bond of terminal alkynes, pyridazines and pyrimidine equipped with the

PIP substituent were alkynylated in moderate yields (Scheme 6).<sup>17</sup>



**Scheme 5** Nickel-catalyzed alkylation of diazines directed by chelating group (top) and plausible reaction mechanism (bottom). Ni =  $\text{NiCl}_2$  (10 mol%).



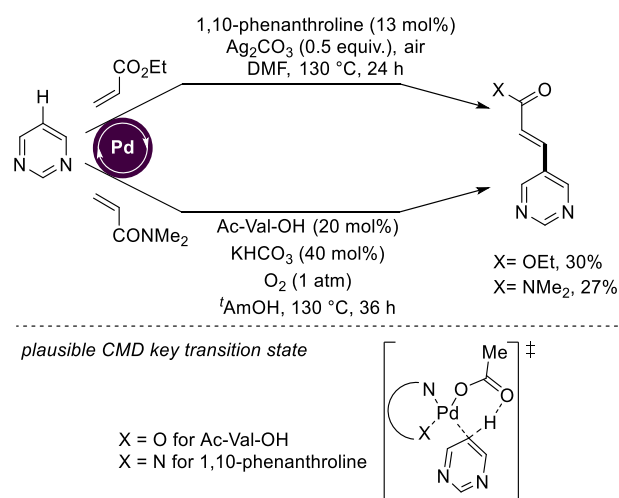
**Scheme 6** Copper-catalyzed alkylation of diazines directed by a chelating group. Cu =  $\text{Cu}(\text{OAc})_2$  (30 mol%).

#### 4 Transition metal-catalyzed C-H alkenylation of diazines

There are essentially two types of reactions to connect an olefinic substituent to an aromatic core: either i) cross coupling with an olefin described as a dehydrogenative Heck reaction or ii) hydroarylation of alkynes, both methods involving C-H bond activation and C-C bond formation. Complexes of palladium, rhodium and ruthenium are the catalysts of choice for these activations, but a few examples with 3d metals such as Ni and Co have also been reported.

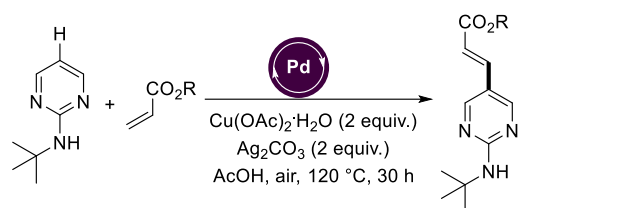
#### 4.1 Alkenylation with olefins

The alkenylation of pyrimidine with the electron-deficient ethyl acrylate<sup>18</sup> and dimethylacrylamide<sup>19</sup> has been initially carried out with 10 mol% of  $\text{Pd}(\text{OAc})_2$  associated with 1,10-phenanthroline or a *N*-protected amino acid such as Ac-Val-OH and  $\text{Ag}_2\text{CO}_3$  and/or air as oxidant. In both cases, selective alkenylation took place selectively at the C5 position of the pyrimidine but modest yields below 30% were obtained (Scheme 7, top). The origin of the regioselectivity towards olefination at the C5 position was studied by DFT calculations identifying the C-H activation step via concerted-metalation deprotonation (CMD) as the rate-determining one (Scheme 7, bottom).<sup>19</sup> Functionalization at the other C-H bonds was more energetically demanding likely due to the influence of the ligands coordinating to palladium.



**Scheme 7** Palladium-catalyzed alkenylation of pyrimidine (top) and plausible key intermediate (bottom). Pd =  $\text{Pd}(\text{OAc})_2$  (10 mol%).

Improved productivities were obtained from 2-aminopyrimidines with a catalytic system based on palladium(II) acetate avoiding the use of external ligand but operating in air in the presence of additional copper acetate as oxidant in acetic acid as solvent at 120 °C. With this procedure, excellent yields of 5-alkenylated pyrimidines of biological interest could be obtained in excellent yields (Scheme 8, top).<sup>20</sup> The regio-selectivity of this reaction is imposed by a dearomatization at the substrate occurring simultaneously to the electrophilic C-H palladation (Scheme 8, bottom). A Heck-type process is operative in which migratory insertion of the olefin follows  $\beta$ -hydride *syn* elimination forming the product and palladium-hydride species. Reductive elimination at palladium forms acetic acid and palladium(0) that is chemically oxidized with copper salts (Scheme 8, bottom). A related catalytic system containing silver acetate as oxidant and pivalic acid made possible the selective monoalkenylation of 2,6-dimethylpyrazine with *tert*-butyl acrylate at 140 °C in DMF in 52% yield.<sup>21</sup>

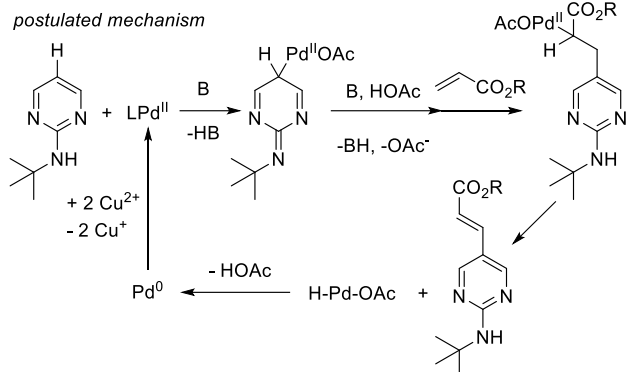


R = Me, Et, <sup>n</sup>Bu, Bn (75-77%)

R = Ph (60%), 4-Me-C<sub>6</sub>H<sub>4</sub> (54%), 4-Br-C<sub>6</sub>H<sub>4</sub> (67%)

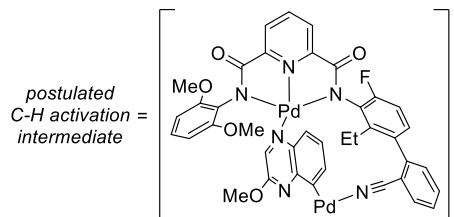
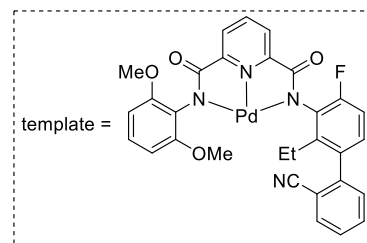
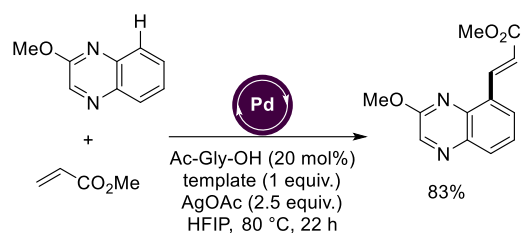
R = CH<sub>2</sub>-4-CF<sub>3</sub>-C<sub>6</sub>H<sub>4</sub> (82%), CH<sub>2</sub>-4-F-C<sub>6</sub>H<sub>5</sub> (68%), CH<sub>2</sub>-3-Cl-C<sub>6</sub>H<sub>4</sub> (60%)

postulated mechanism

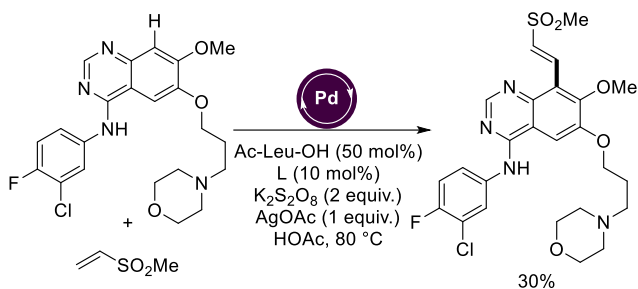


**Scheme 8** Palladium-catalyzed alkenylation of 2-aminopyrimidines (top) and plausible reaction mechanism (bottom).. Pd = Pd(OAc)<sub>2</sub> (10 mol%).

Fused bicyclic diazines have also been alkenylated with electron-deficient olefins with palladium catalysts. With the help of a designed U-shaped template (1 equiv.) added to Pd(OAc)<sub>2</sub> (10 mol%), *N*-protected glycine Ac-Gly-OH (20 mol%), and AgOAc (2.5 equiv.), the regioselective alkenylation of 2-methoxyquinoxaline with methyl acrylate was achieved at 80 °C in hexafluoroisopropanol at 80 °C forming the corresponding 8-alkenylated quinoxaline in 83% yield (Scheme 9).<sup>22</sup> In this case, the regio-selectivity of the reaction is controlled by the use of the ability of the U-shaped template to bind in a ditopic fashion the substrate via Pd...N interaction and the palladium active site via nitrile...Pd interaction. The geometry and distance between the substrate binding site and the catalytically active palladium site enables the formation of large palladacycle species responsible of such precise regio-selectivity. A highly functionalized quinazoline has been alkenylated by methyl vinyl sulfone in the presence of a complex catalytic system based on Pd(CF<sub>3</sub>CO<sub>2</sub>)<sub>2</sub> (10 mol%) operating under strong oxidative conditions in the presence of 2 equiv. of potassium persulfate. A late stage functionalization the anti-cancer drug gefitinib was thus obtained in 30% yield (Scheme 10).<sup>23</sup>



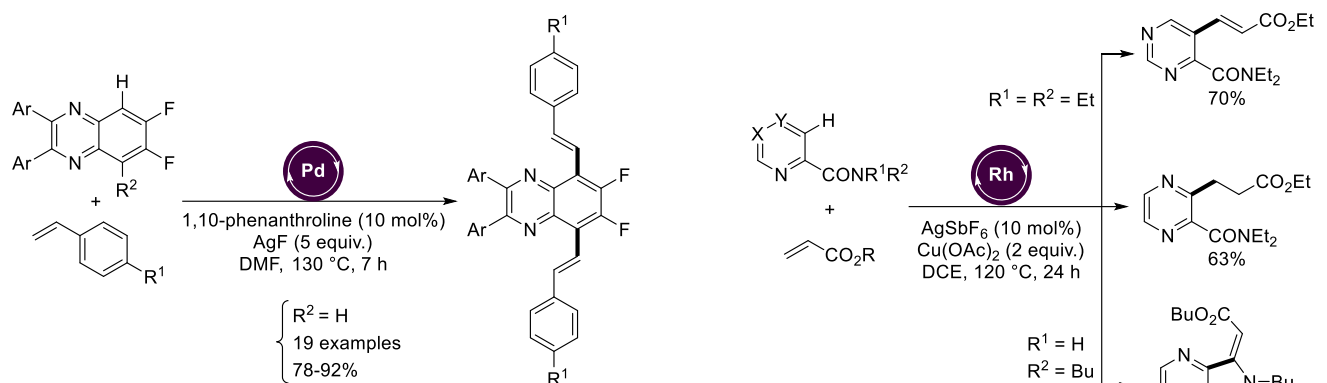
**Scheme 9** Template-enabled remote C-H olefination of a quinoxaline derivative under palladium catalysis (top) and postulated key palladacycle intermediate (bottom). Pd = Pd(OAc)<sub>2</sub> (10 mol%).



**Scheme 10** C-H olefination of Gefitinib under palladium catalysis. L = 3-methyl-2-isopropyl-2-(phenylthio)acetic acid. Pd = Pd(CF<sub>3</sub>CO<sub>2</sub>)<sub>2</sub> (10 mol%).

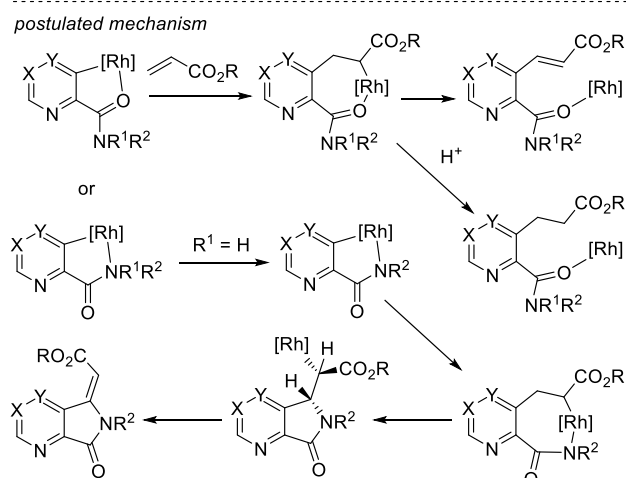
Styrenes are also convenient substrates to perform the alkenylation of diazines. This has been demonstrated in the olefination of 6,7-difluoroquinoxalines by styrenes with extended electronic conjugation leading to fluorophores with high potential for bioimaging applications. The palladium catalyst consisted in Pd(CF<sub>3</sub>CO<sub>2</sub>)<sub>2</sub> (5 mol%), 1,10-phenanthroline (10 mol%), and AgF (5 equiv.) working in DMF at 130 °C for 7 h. Depending on the substitution pattern at position 5 of the initial quinoxaline, symmetrical and unsymmetrical molecules were obtained in excellent yields (Scheme 11).<sup>24</sup> The reaction appears to undergo a Fujiwara-Moritani-type mechanism although no discussion was reported.





**Scheme 11** C-H olefination of 6,7-difluoroquinoxalines with styrenes under palladium catalysis. Pd = Pd(TFA)<sub>2</sub> (5 mol%).

Whereas the alkylation of diazines was selectively achieved at the vicinal carbon of nitrogen atoms in the presence of rhodium(I) catalysts, their alkenylation was possible with rhodium(III) catalysts but required the presence of a directing group. However, the reaction of simple diazines with acrylates was sensitive to the nature of the diazine and the directing group. For instance, with [Cp\**Rh*Cl<sub>2</sub>]<sub>2</sub> as catalyst precursor, AgSbF<sub>6</sub> as chloride abstractor and Cu(OAc)<sub>2</sub> as oxidant, a tertiary amide at C4 position of pyrimidine led to the alkenylation at C5 in 70% yield with ethyl acrylate whereas the same directing group at the C2 position of pyrazine gave the alkylation at C3 in 63% yield (Scheme 12, top).<sup>25</sup> In contrast when the pyrazine was substituted by a secondary amide at the same position, a further cyclization which required both the presence of rhodium and copper catalysts was observed in 43% yield (Scheme 12, top).<sup>26</sup> In these cases, the key rhodacycle intermediate is the same with a β-hydride elimination step explaining the olefinated product whereas a protonation step instead leads to the alkylated product (Scheme 12, bottom). The olefinated/cyclized product accounts from a N-H deprotonation after olefination and a syn-addition of the olefin that explains the formation of the *E* isomer after β-hydride elimination (Scheme 12, bottom). The Cu(II) salt enables oxidation of Rh(I) to the catalytically active Rh(III).

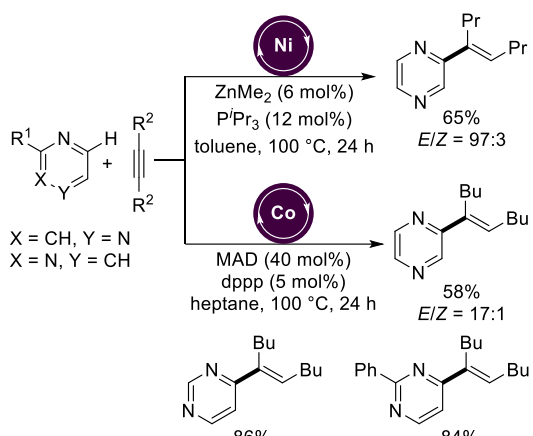


**Scheme 12** Amide-directed C-H olefination of pyrimidine, C-H alkylation of pyrimidine and C-H olefination/cyclization of pyrazine derivatives under rhodium catalysis (top) and key mechanistic considerations (bottom). Rh = [Cp\**Rh*Cl<sub>2</sub>]<sub>2</sub> = (2.5 mol%).

#### 4.2 Alkenylation with alkynes

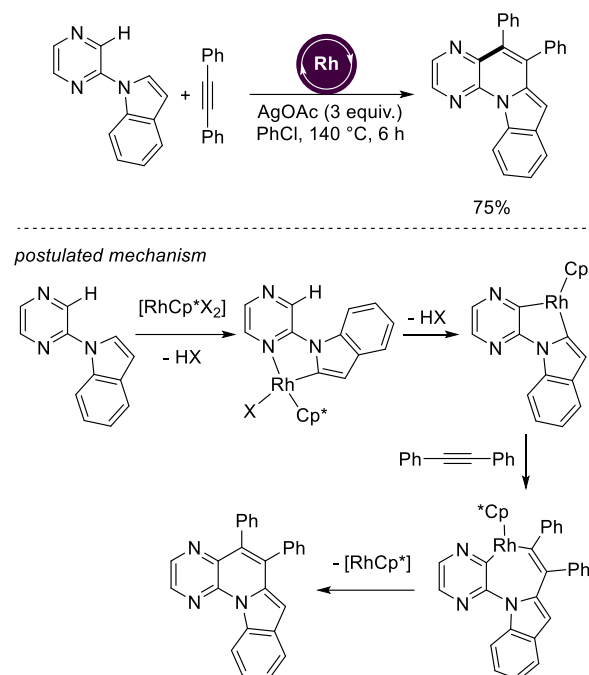
With alkynes as coupling partners alkenylation of non-substituted monocyclic diazines, namely pyrazine and pyrimidine, leads to the introduction of a linear olefinic substituent. On the other hand, diazines which are substituted by an (hetero)aromatic group in most cases give cyclized products with formation of two C-C bonds or an additional C-heteroatom bond. The first example of diazine alkenylation *via* transition metal catalysis was reported in 2008. Pyrazine reacted with 1,2-dipropylethyne in the presence of catalytic amounts of two metal catalysts, Ni(cod)<sub>2</sub> (3 mol%) and ZnMe<sub>2</sub> (6 mol%), and P<sup>*i*</sup>Pr<sub>3</sub> (12 mol%) in toluene at 100 °C. 2-(1-propylpent-1-en-1-yl)pyrazine was selectively obtained in 65% yield with a *E/Z* stereoisomer ratio of 97/3 (Scheme 13). In this process, the Ni(0) catalyst activates the triple bond and the pyridine is activated by the zinc Lewis acid facilitating the regioselective oxidative addition of the C2-H bond of pyrazine to form a nickel(II) intermediate.<sup>27</sup> It can be noted that a second molecule of alkyne could be involved forming a 1,2,3,4-tetrapropylbutadien-1-yl

substituted pyrazine in 10% with  $\text{ZnMe}_2$  that could become the major product using  $\text{AlMe}_3$  as Lewis acid. Later on, the  $\text{Co}(\text{acac})_3$  complex associated with dppp (5 mol%) and  $\text{MeAl}(\text{2,6-di}^t\text{Bu-4-MeC}_6\text{H}_2\text{O}_2)_2$  (MAD) as Lewis acid was found very efficient for the same alkenylation reaction of pyrazine at C2 position and pyrimidine at C5 position (Scheme 13).<sup>28</sup> In both cases, the Lewis acid ( $\text{ZnMe}_2$  or MAD) is expected to bind to the nitrogen atom of the heteroaromatic ring leading to a C-H metalation step followed by hydrometallation across the alkyne coordinating to the metal center and further reductive elimination as the plausible reaction mechanism.



**Scheme 13** C-H alkenylation of diazines with alkynes under nickel catalysis and under cobalt catalysis, respectively (top) and plausible reaction mechanism (bottom). Ni =  $\text{Ni}(\text{cod})_2$  (3 mol%). Co =  $\text{Co}(\text{acac})_3$  (5 mol%).

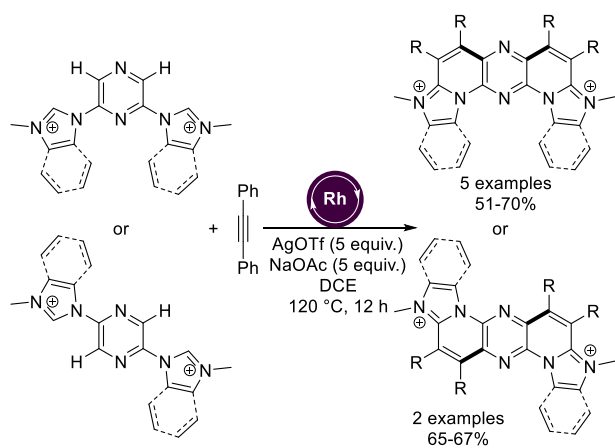
Several groups have shown that rhodium(III) catalysts were able to promote the dehydrogenative coupling/annulation of pyrazines with internal alkynes.<sup>29-31</sup> Starting from a pyrazine core substituted by a proximal indole, the reaction with diphenylacetylene provided a tetracyclic heteroaromatic in 75% yield in the presence of 4 mol% of  $[\text{Cp}^*\text{RhCl}_2]_2$  and 3 equiv. of silver acetate as oxidant (Scheme 14, top).<sup>29</sup> This reactivity has been explained by first rhodium-mediated C-H bond activation of indole directed by coordination of one nitrogen atom of the pyrazine to form a rhodacycle followed by insertion of the triple bond, rollover cyclorhodation and elimination (Scheme 14, bottom).



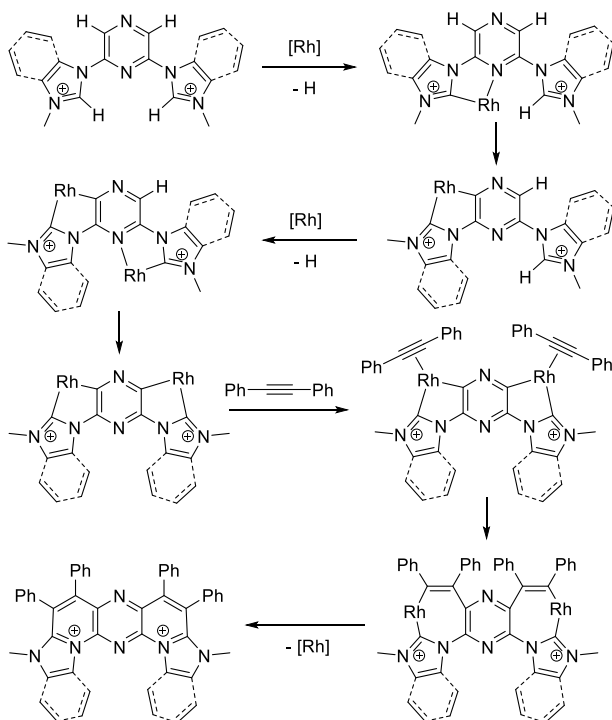
**Scheme 14** C-H dehydrogenative/cyclizing alkenylation of a pyrazine derivative under rhodium catalysis (top) and plausible reaction mechanism (bottom). Rh =  $[\text{Cp}^*\text{RhCl}_2]_2$  (4 mol%).

The same strategy based on a rollover mechanism was extended to pyrazines disubstituted by imidazole and imidazolium motifs in positions 2,6 and 2,5 to form highly condensed conjugated systems with fluorescence properties. The catalytic system containing silver triflate and sodium acetate was active for the imidazolium and benzimidazolium salts whereas  $\text{Cu}(\text{OAc})_2$  was more efficient for the neutral imidazole salts (Scheme 15, top).<sup>30</sup> The reaction mechanism is similar to the one described before but involving a 4 C-H bond activation events thanks to rhodium, 2 rollovers and 2 annulations (Scheme 15, bottom).





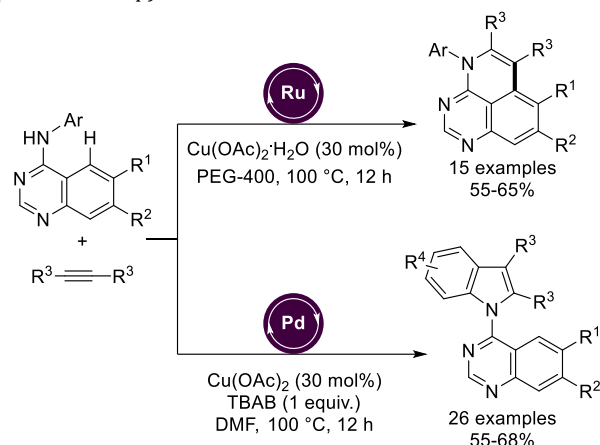
postulated mechanism



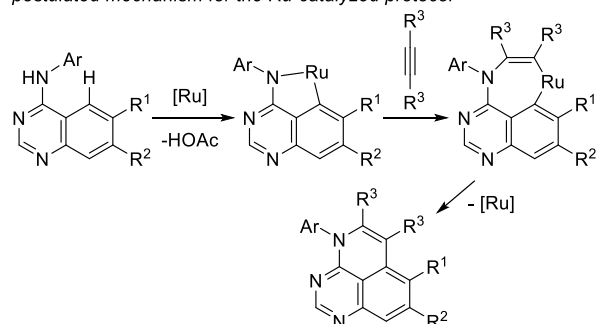
**Scheme 15** C-H dehydrogenative/cyclizing alkenylation of pyrazine imidazolium salts with alkynes under rhodium catalysis (top) and plausible reaction mechanism (bottom). Rh =  $[\text{Cp}^*\text{RhCl}_2]_2$  (3 mol%).

The cross dehydrogenative coupling of 4-*N*-arylquinazolines with internal alkynes offers an excellent example of site-selectivity in C-H bond activation/annulation controlled by the catalytic system. The *ortho* C-H selective annulation on the aniline fragment was observed with a palladium catalyst in DMF giving indole-quinazoline, whereas a ruthenium catalyst in PEG-400 provided the annulation at the *peri* C-H bond of the quinazoline ring to furnish pyrido-quinazoline (Scheme 16, top). This is due to the difference of directing groups in the two catalytic systems. With palladium, a six-membered palladacycle was formed with the quinazoline as directing group activating the aniline *ortho*-C-H bond. With ruthenium the formation of the five-membered ruthenacycle upon activation of the *peri*-C-H bond of the quinazoline directed by the amino group of aniline was favored (Scheme 16, bottom). In both cases, broad scope of alkynes and substituted quinazolines were evidenced and the

different families of products corresponding to concomitant C-C and C-N bond formation were obtained in 55-68% yields (Scheme 16, top).<sup>31</sup>



postulated mechanism for the Ru-catalyzed protocol



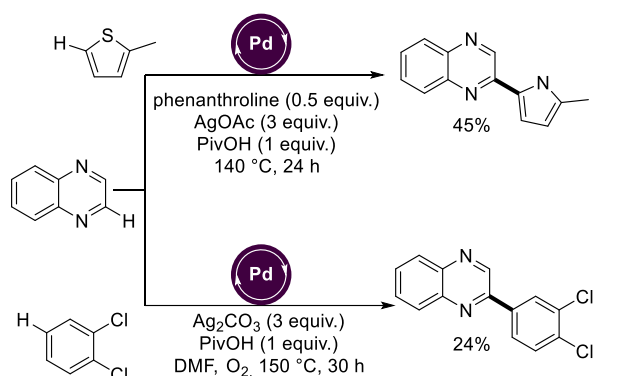
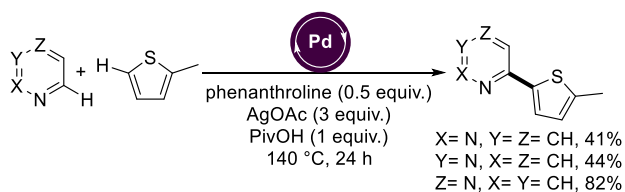
**Scheme 16** Site-selective dehydrogenative cyclizing coupling of 4-*N*-arylquinazolines and alkynes under palladium and ruthenium catalysts (top) and plausible reaction mechanism for the ruthenium-catalyzed methodology (bottom). Ru =  $[\text{RuCl}_2(p\text{-cymene})]_2$  (5 mol%). Pd =  $\text{Pd}(\text{OAc})_2$  (10 mol%).

## 5. Transition metal-catalyzed arylation of diazines

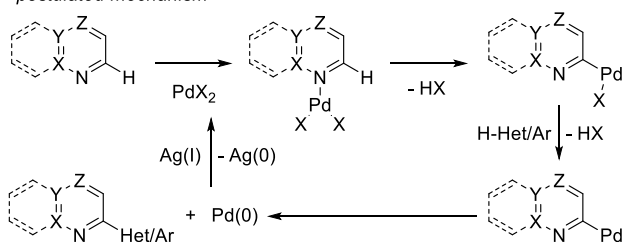
Two strategies have been investigated to perform the diazines (hetero)arylation *via* C-H bond activation in the presence of transition metal catalysts: (i) the oxidative C-H/C-H cross coupling of diazines with (hetero)arenes directly from non-activated substrates, which represents the most attractive approach from an atom- and step-economy point of view,<sup>32</sup> and (ii) the (hetero)arylation with (pseudo)halides

### 5.1 Metal-catalyzed arylation *via* oxidative coupling

The first dehydrogenative cross coupling of diazines involved 2-methylthiophene as coupling partner in the presence of palladium(II) associated with a phenanthroline ligand, pivalic acid as proton shuttle and silver acetate as oxidant to close the catalytic cycle (Scheme 17, top).<sup>33</sup> With this catalytic system using a large excess of diazine as solvent, diazines were selectively arylated at the  $\alpha$ -position of one nitrogen atom, pyrazine being more reactive than pyrimidine and pyridazine. Quinoxaline was arylated by 2-methylthiophene in 45% yield under the same conditions. Other catalytic conditions avoiding the *N,N*-chelating ligand and working under air at higher temperature gave only 24% yield for the oxidative coupling with 1,2-dichlorobenzene (Scheme 17, top).<sup>34</sup> The reaction mechanism for this type of reactions involves initial coordination of the nitrogen from the diazine to the palladium catalyst followed by a palladium shift/deprotonation at the neighboring alfa position. A *trans*-effect at palladium is also postulated for enabling  $\eta^6$  binding of the substrate to the palladium. Next, electrophilic palladation with the coupling partner H-Het/Ar precedes the reductive elimination and the formed palladium(0) species are in situ oxidized with silver(I) salts.



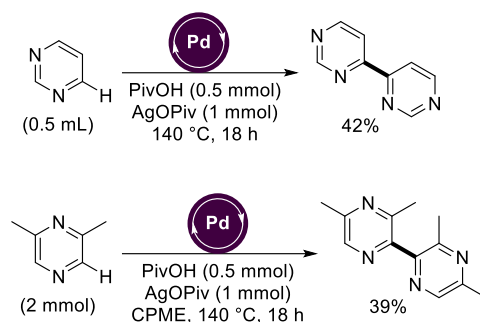
postulated mechanism



**Scheme 17** Oxidative C-H/C-H cross-coupling of diazines enabling formal (hetero)arylation under palladium catalysis (top) and plausible reaction mechanism (bottom). Pd = Pd(OAc)<sub>2</sub> (10 mol%).

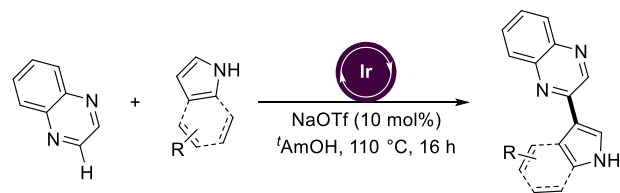
The system consisting in palladium acetate/silver pivalate/pivalic acid was also shown to be efficient for the oxidative homo-coupling of diazine derivatives at 140 °C (Scheme 18). The C-C coupling took place at a vicinal carbon with

respect to a nitrogen atom, more precisely at C4 position of pyrimidine and C2 position of 2,6-dimethylpyrazine to give the corresponding 2,2'-bis-diazines in 42 and 39% yield, respectively.<sup>35</sup> The selectivity for these examples is explained as just above discussed in Scheme 17 (bottom).

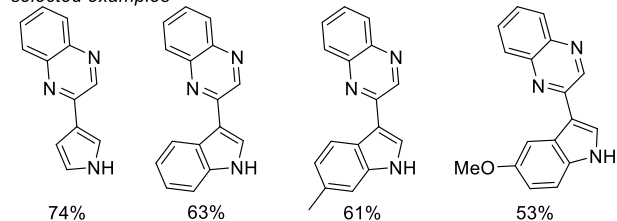


**Scheme 18** Oxidative C-H/C-H homo-coupling of diazines enabling formal (hetero)arylation under palladium catalysis. Pd = Pd(OAc)<sub>2</sub> (0.1 mmol).

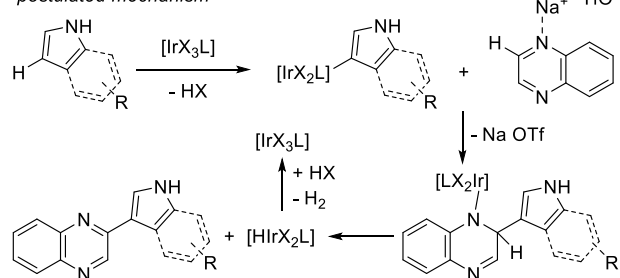
Besides palladium catalysts, the iridium(III) complex [IrCp\*Cl<sub>2</sub>]<sub>2</sub> in the presence of Na OTf in *tert*-amyl alcohol has made possible the oxidative coupling of pyrrole and indoles with quinoxaline under mild conditions at 110 °C. The new C-C bond connected the C2 position of the diazine and the C3 position of cross coupling partner (Scheme 19, top).<sup>36</sup> In this case, the reaction begins with C-H functionalization at the most acidic indole C3 site whereas the sodium triflates activates the C2 site of the diazine that undergoes carbon-carbon bond formation followed by  $\beta$ -hydride elimination and regeneration of the catalytically active iridium(III) species with concomitant formation of H<sub>2</sub> at each catalytic cycle (Scheme 19, bottom).



selected examples



postulated mechanism

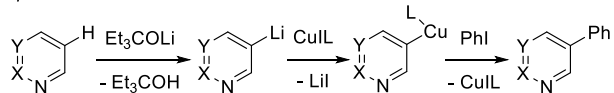
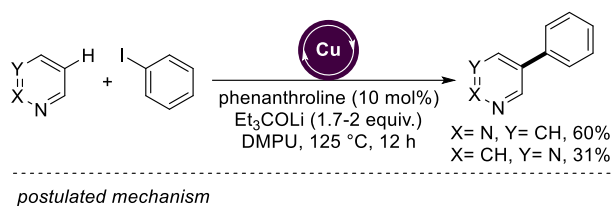


**Scheme 19** Oxidative C-H/C-H coupling of quinoxaline enabling formal (hetero)arylation under iridium catalysis (top) and

plausible reaction mechanism (bottom). Ir = [IrCp\*Cl<sub>2</sub>]<sub>2</sub> (1 mol%).

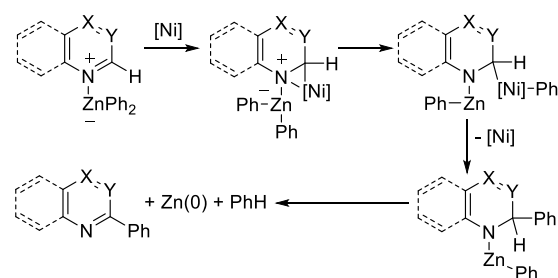
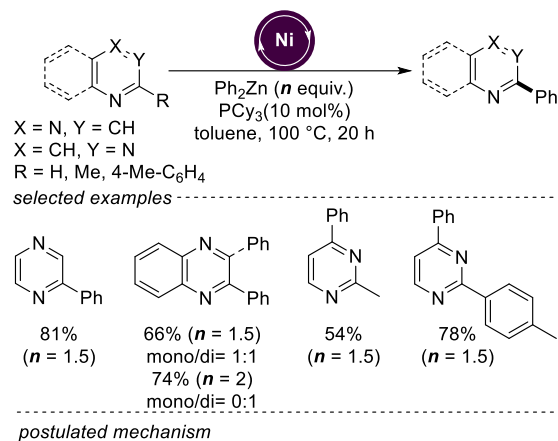
## 5.2 Metal-catalyzed arylation *via* coupling with (pseudo)aryl coupling partners

The interest of biaryl derivatives in various applications has triggered the search for efficient synthesis strategies. Indeed, arylation of *N*-heterocyclic substrates based on C-H bond activation was rapidly investigated as soon as efficient transition metal catalysts were discovered for arylation of aromatics.<sup>37</sup> In 2008, a copper iodide/phenanthroline catalytic system performed the first phenylation of pyrimidine and pyridazine by phenyl iodide in the presence of Et<sub>3</sub>COLi as a base in *N,N'*-dimethylpropylene urea (DMPU) at 125 °C. The more acidic C-H bond of the diazine was activated leading to the formation of an organocopper(I) intermediate at C4 for pyridazine and C5 for pyrimidine (Scheme 20, top).<sup>38</sup> The best yield obtained with pyridazine was attributed to the higher acidity of the C4 proton. The mechanism operating likely involves base-assisted C-H metalation followed by copper transmetalation and Ullmann-type arylation (Scheme 20, bottom). Related versions with CuCl<sub>2</sub> and MnCl<sub>2</sub> as the pre-catalysts, respectively, have been reported.<sup>39,40</sup>



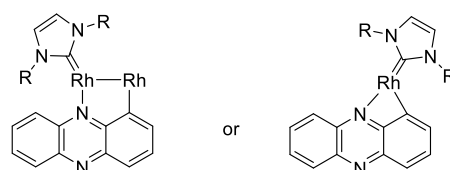
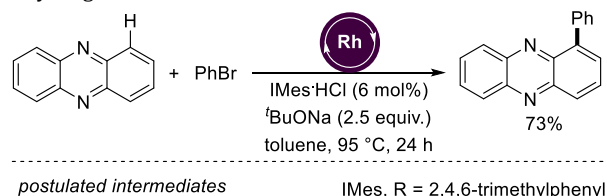
**Scheme 20** C-H arylation of pyridazine and pyrimidine under copper catalysis (top) and plausible reaction mechanism (bottom). Cu = CuI (10 mol%).

Then, mono- and di-arylation of pyrazine and quinoxaline were achieved in good yields with Ph<sub>2</sub>Zn as aryl source in the presence of the nickel(0) precursor Ni(cod)<sub>2</sub> associated with PCy<sub>3</sub> (Scheme 21, top).<sup>41</sup> In this reaction, the formation of intermediate 3,4-dihydropyrimidine has been observed (Scheme 21, bottom), which orientated the mechanism towards first formation of an azanickelacyclopropane that undergoes transmetalation with diphenylzinc rather than a direct C-H bond activation *via* classical deprotonation or oxidative addition.



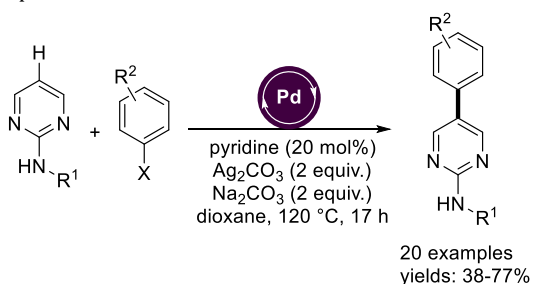
**Scheme 21** C-H arylation of pyrazine and quinoxaline under nickel catalysis. Ni = Ni(COD)<sub>2</sub> (5 mol%).

Rhodium(I) complexes already mentioned in alkylation of diazines also promoted arylation of diazines at vicinal positions of nitrogen in these heterocycles. Disappointingly, the arylation of 2,3-dimethylpyrazine and 4,6-dimethylpyrimidine with 2-bromonaphthalene at 175 °C for 24 h led to only 26 and 33% yield, respectively.<sup>42</sup> On the other hand, catalytic amounts of Rh<sub>2</sub>(OAc)<sub>4</sub> and 1,3-bis(mesityl)imidazolium chloride (IMes.HCl) in the presence of 2.5 equiv. of <sup>t</sup>BuONa allowed the mono-arylation at a *peri*-position of phenazine, an extended quinoxaline structure, with phenyl bromide in 73% yield (Scheme 22, top).<sup>43</sup> Although no mechanistic cycle was proposed, key rhodacycle species either dimeric or monomeric for the C-H activation step were postulated (Scheme 22, bottom). It must be underlined that the catalytic system [RhCl(coe)]<sub>2</sub>/PCy<sub>3</sub>/NEt<sub>3</sub> could not achieve the phenylation of quinazoline with PhI at 150 °C in THF, whereas under similar conditions it directly gave 2-phenylquinazoline in 78% yield from 3,4-dihydroquinazoline, probably *via* cross-coupling giving phenyldihydroquinazoline followed by dehydrogenative aromatization.<sup>42</sup>



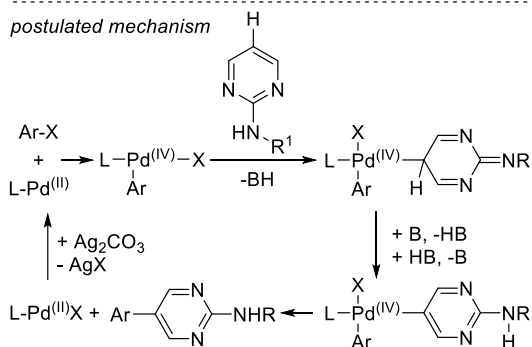
**Scheme 22** C-H arylation of phenazine under rhodium catalysis (top) and key rhodacycle species involved in the C-H activation step (bottom). Rh = Rh<sub>2</sub>(OAc)<sub>4</sub> (3 mol%).

Palladium catalysis proved very efficient for diazine arylation based on coordination of a nitrogen atom and/or the easy deprotonation of specific acidic protons of these *N*-heterocycles without introduction of a directing group orientating the C-H bond activation. For instance, 2-aminopyrimidines have been arylated with aryl halides in the presence of palladium acetate as catalyst precursor associated with pyridine as ligand, sodium carbonate as a base and silver carbonate as halide abstractor (Scheme 23, top).<sup>20</sup> The reaction tolerated both electron-donating and -withdrawing groups on the aryl group. It was assumed to proceed *via* a Pd(II)/Pd(IV) catalytic cycle with initial oxidative addition involving the aryl halide and subsequent C-H activation involving a dearomatization followed by base-assisted aromatization ending with a reductive elimination and regeneration of the active palladium(II) species upon reaction with silver salts (Scheme 23, bottom). However, only secondary amines were reactive, which suggested that the carbonate-assisted deprotonation of the amino group enhanced the electronic density at the C5 position favoring the palladation at this position.



R<sup>1</sup> = Me, <sup>i</sup>Pr, Cy, <sup>t</sup>Bu, 3-C<sub>6</sub>H<sub>11</sub>, CH<sub>2</sub>CH<sub>2</sub>Ph  
 R<sup>2</sup> = H, *p*-Me, 3,5-Me<sub>2</sub>, 4-<sup>t</sup>Bu, 4-OMe, 3-OMe  
 4-Cl, 3-Cl, 3-F, 4-CF<sub>3</sub>, 3-CF<sub>3</sub>, 4-NO<sub>2</sub>, 4-CO<sub>2</sub>Et  
 X = I, Br, Cl

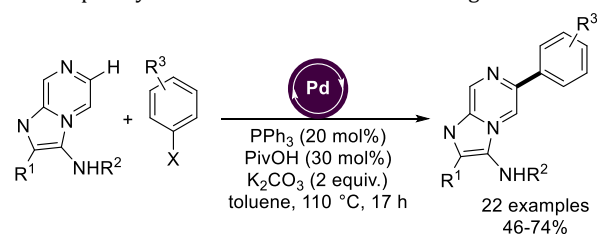
postulated mechanism



**Scheme 23** C-H 5-arylation of 2-aminopyrimidines under palladium catalysis (top) and plausible reaction mechanism (bottom). Pd = Pd(OAc)<sub>2</sub> (10 mol%), B = base.

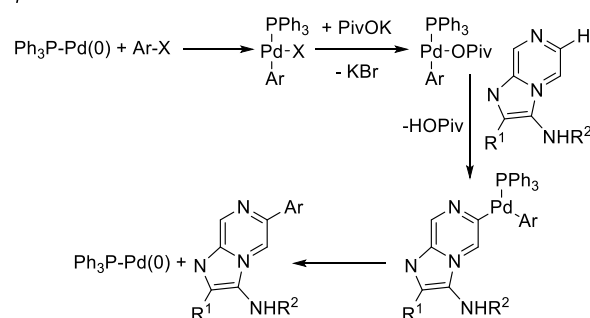
Condensed 3-aminoimidazo[1,2-*a*]pyrazines have been regioselectively arylated at the vicinal carbon atom of the pyrazine ring which is not involved in the bicyclic structure. The catalytic system was based on palladium acetate and triphenylphosphine in the presence of pivalic acid and potassium carbonate (Scheme 24, top).<sup>44</sup> Aryl bromides in excess (2.5

equiv.) were used as arylating agent leading to a variety of C6-arylated in 46-74% yields. The mechanism of the reaction involves initial formation of palladium(II) species upon oxidative addition with aryl halide followed by halide/carboxylate exchange at palladium and concerted metalation deprotonation at the most acidic C-H bond from the diazine substrate finishing with reductive elimination and regeneration of palladium(0) species (Scheme 24, bottom). It is noteworthy that when R<sup>1</sup> (Scheme 24, top) was an aromatic ring, arylation could also take place at the *ortho*-position of this group depending on the nature of the catalytic system, but the use of PPh<sub>3</sub> as ligand and pivalic acid completely inhibited the formation of this regioisomer.



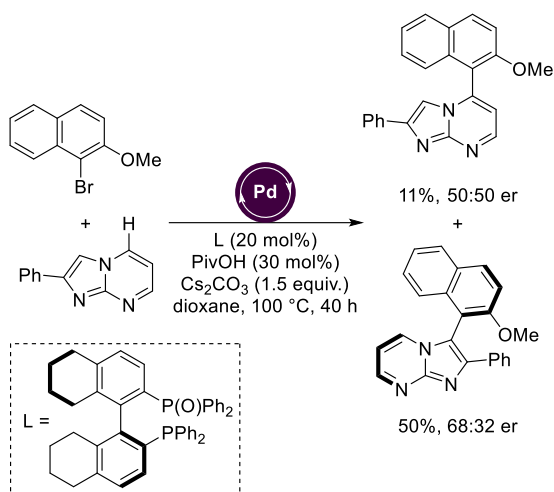
R<sup>1</sup> = C<sub>6</sub>H<sub>5</sub>, 4-ClC<sub>6</sub>H<sub>4</sub>, 4-MeOC<sub>6</sub>H<sub>4</sub>, 2-naphthyl, <sup>n</sup>Pr  
 R<sup>2</sup> = <sup>t</sup>Bu, <sup>n</sup>Bu, Cy, 4-MeO-C<sub>6</sub>H<sub>4</sub>, 3,4,5-(MeO)<sub>3</sub>C<sub>6</sub>H<sub>2</sub>  
 R<sup>3</sup> = H, 4-Me, 4-Cl, 4-F, 4-CN, 4-NO<sub>2</sub>, 4-CHO, 4-MeO

postulated mechanism



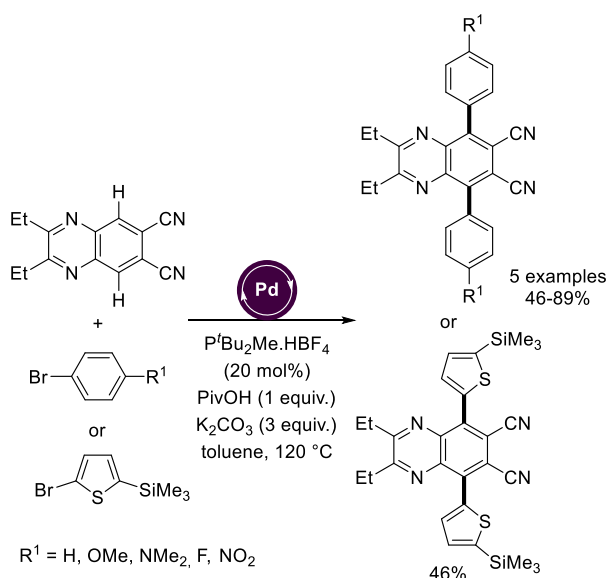
**Scheme 24** C-H arylation of imidazopyrazines under palladium catalysis (top) and plausible reaction mechanism (bottom). Pd = Pd(OAc)<sub>2</sub> (10 mol%).

A related catalytic system using an optically pure bidentate phosphine-phosphine oxide ligand produced a racemic mixture of C4-arylated 2-phenylimidazo[1,2-*a*]pyrimidine in 11% yield as a side product, the major product obtained in 50% yield (in 68:32 enantiomeric ratio) resulting from arylation of the imidazole ring (Scheme 25).<sup>45</sup>

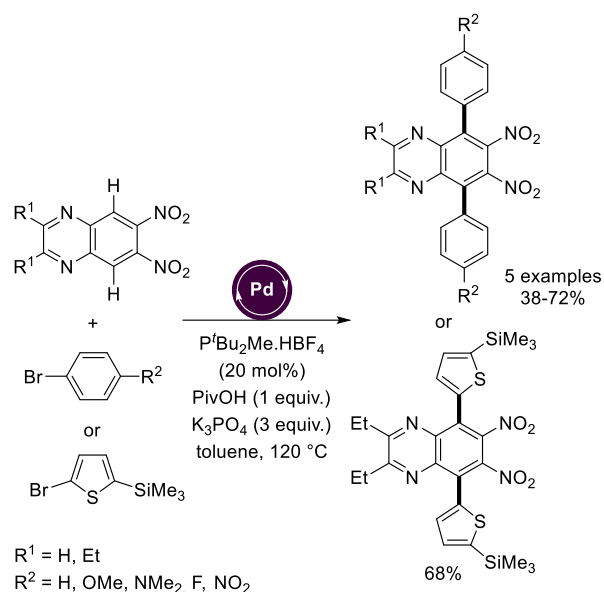


**Scheme 25** C-H arylation of an imidazopyrimidine derivative under palladium catalysis. Pd = Pd(OAc)<sub>2</sub> (10 mol%).

Quinoxalines bearing cyano groups in the neighboring aromatic C6 and C7 positions readily undergo selective C-H bis-arylation at the C5 and C8 positions under palladium catalysis in the presence of aryl bromides as coupling partners (Scheme 26).<sup>46</sup> The most appropriate catalytic system was Pd(OAc)<sub>2</sub> as the catalyst precursor and P<sup>t</sup>Bu<sub>2</sub>Me as the ligand in a 1:2 ratio together with a combination of pivalic acid and potassium carbonate in excess. Modified reactions by replacing the palladium precursor for Pd<sub>2</sub>dba<sub>3</sub> and the base for potassium phosphate enabled the same type of reactivity with quinoxalines substituted with nitro groups in positions C6 and C7 (Scheme 27). These reactions were compatible with thiophene as the heteroaryllating source. These methodologies afforded poly(hetero)aromatic products relevant for materials science as they are strong electron acceptors.

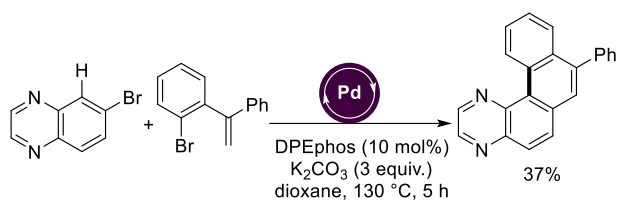


**Scheme 26** C-H arylation of dicyanoquinoxaline derivatives under palladium catalysis. Pd = Pd(OAc)<sub>2</sub> (10 mol%).

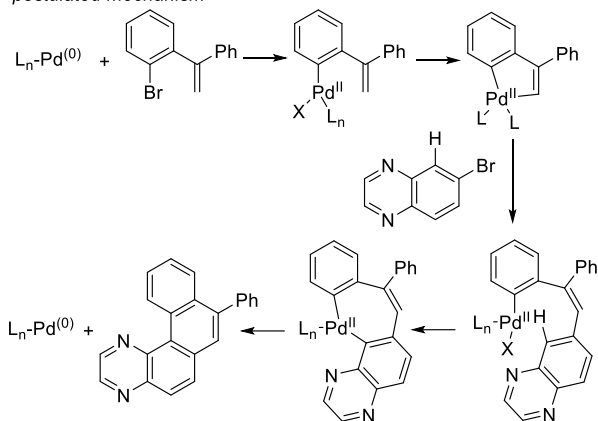


**Scheme 27** C-H arylation of dinitroquinoxaline derivatives under palladium catalysis. Pd = Pd<sub>2</sub>dba<sub>3</sub> (10 mol%).

A quinoxaline scaffold brominated in C7 position was found to undergo a sequence of cross-coupling and annulation with an *ortho*-vinyl bromobenzene partner under palladium catalysis leading an original poly(hetero)aromatic system (Scheme 28, top).<sup>47</sup> The authors demonstrated the importance of using bis[(2-diphenylphosphino)phenyl]ether (DPEphos) as the ligand yet the product was formed in a poor yield. The reaction mechanism (Scheme 29, bottom) likely operates by first reacting with the *ortho*-vinyl bromobenzene reagent *via* oxidative addition at palladium followed by an intramolecular C-H activation and formation of a five-membered ring palladacycle, which has been characterized by the authors. A Heck-type event occurs between the palladium ligated olefin and the carbon-bromide bond from the diazine leading to the arylated olefin backbone which places the C-H bond at the C8 position from the benzodiazine nearby the palladium for enabling a second C-H activation step. Final reductive elimination affords the final product with concomitant formation of palladium(0) species.

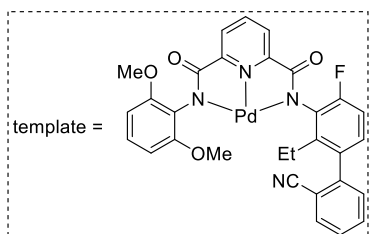
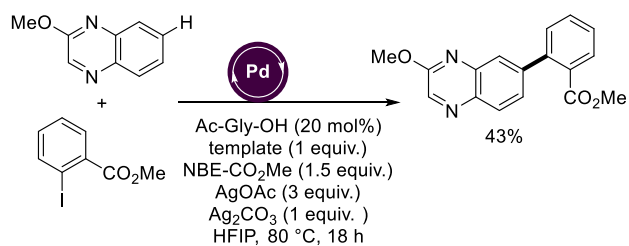


postulated mechanism



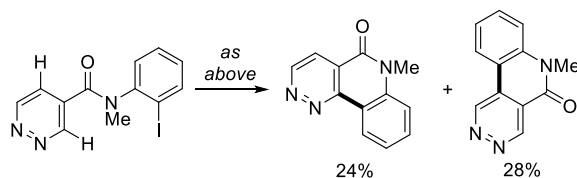
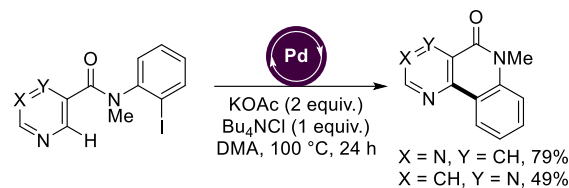
**Scheme 28** Sequential Heck/C-H arylation of 7-bromoquinoxaline under palladium catalysis (top) and plausible reaction mechanism (bottom). Pd = Pd(OAc)<sub>2</sub> (5 mol%).

In 2020, the Yu group reported a palladium tridentate template comprising a nitrile group that enabled the selective C-H arylation in remote positions of heterocycles under palladium catalysis.<sup>48</sup> Particularly, by means of a mediator (NBE-CO<sub>2</sub>Me, NBE = norbornene) and a very specific set of reagents, it was possible to reach the very challenging C7-arylation of a quinoxaline derivative although in a modest yield of 43% (Scheme 29). The reaction mechanism resembles the action mode already described in Scheme 9 (bottom) but with additional switch in the C-H activation step from C8 to C7 due to a Catellani-type mechanism involving the norbornene derivative.

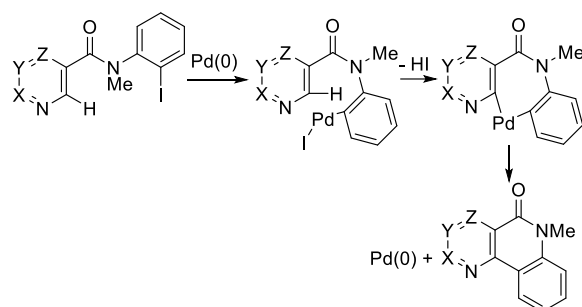


**Scheme 29** Remote C-H arylation of a quinoxaline derivative under palladium catalysis. Pd = Pd(OAc)<sub>2</sub> (10 mol%).

Iodine-containing diazines underwent intramolecular C-H arylation under palladium catalysis provided that amides behaved as *ortho*-directing groups (Scheme 30, top).<sup>49</sup> The C-H arylation in the pyrimidine-containing derivative formed in higher yield (79%) compared to the pyrazine one (49%). In the case of pyridazine a mixture of regioisomers were observed in almost statistical ratio with an overall 52% yield. The reaction is thought to proceed via initial oxidative addition of the carbon-iodine bond into palladium followed by intramolecular C-H activation via the concerted metalation deprotonation pathway. Upon reductive elimination, palladium(0) and the product are formed (Scheme 30, bottom).



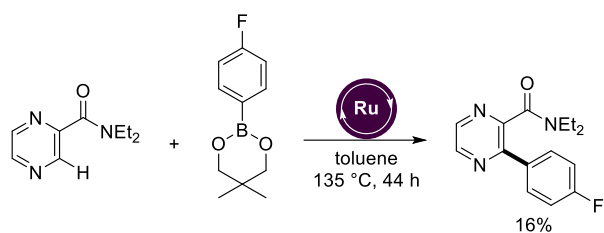
postulated mechanism



**Scheme 30** Intramolecular C-H arylation of anilide-containing diazines under palladium catalysis (top) and plausible reaction mechanism (bottom). Pd = Pd(OAc)<sub>2</sub> (5 mol%).

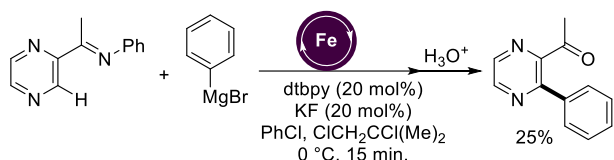
Similarly, a directing group strategy was applied to the ruthenium-catalyzed C-H arylation of a pyrazine derivative (Scheme 31).<sup>50</sup> In this case, the arylating coupling partner is derived from boroneopentylate and a tertiary amide behaved as *ortho*-directing group within the diazine core leading to the C3-arylated product in a poor yield when using RuH<sub>2</sub>(CO)(PPh<sub>3</sub>)<sub>3</sub> as the metal pre-catalyst in toluene solvent.





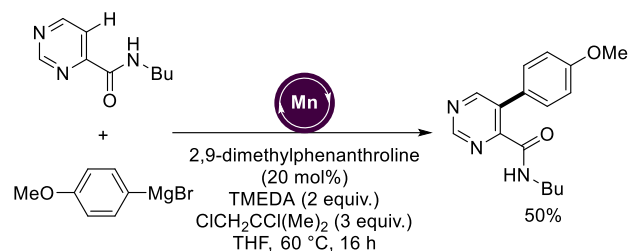
**Scheme 31** Intermolecular C-H *ortho*-arylation of pyrazine by amide chelation under ruthenium catalysis. Ru =  $\text{RuH}_2(\text{CO})(\text{PPh}_3)_3$  (10 mol%).

Analogously, an iron-catalyzed methodology was applied to the selective *ortho*-C-H arylation of pyrazine with an imine group that behaves as directing group (Scheme 32).<sup>51</sup> A bipyridine ligated iron complex is assumed to be the active species and an excess of 6 equivalents of arylating coupling partner were employed with 20 mol% of KF as additive using a mixture of chlorinated solvents. A final hydrolysis step was performed to obtain the ketone-containing diazine derivative in 25% yield.

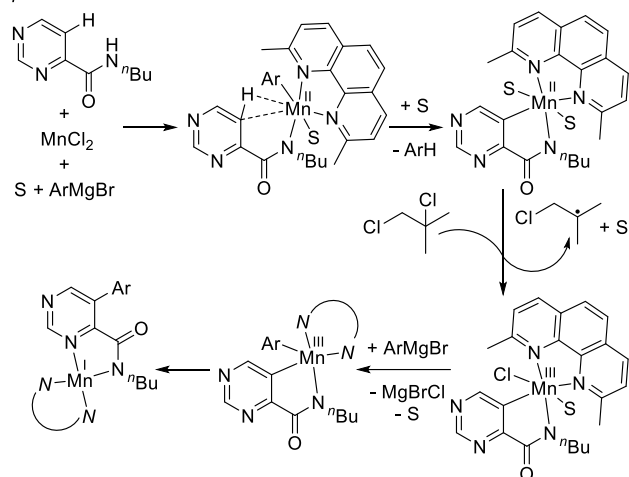


**Scheme 32** Intermolecular C-H *ortho*-arylation of pyrazine by imine chelation under iron catalysis. Fe =  $\text{Fe}(\text{acac})_3$  (10 mol%).

In the same vein, the Ackermann group reported a manganese-catalyzed C-H arylation with secondary amides behaving as *ortho*-directing groups.<sup>52</sup> This protocol was applied to a pyrimidine derivative leading to 50% yield of the corresponding product after 16 hours at 60 °C (Scheme 33, top). Interestingly, similar efficiencies (53% yield) were reached under flow conditions in less than 2 hours at 80 °C. The catalytically active system required the presence of catalytic amounts of  $\text{MnCl}_2$  and a phenanthroline-type ligand in a 1:2 ratio as well as over-stoichiometric amounts of TMEDA and 1,2-dichloro-2-methylpropane. According to computational calculations and experimental data, the reaction mechanism operates via a manganese(II/III/I) catalytic cycle as shown in Scheme 33 (bottom). The role of the tetrahydrofuran solvent is key to stabilize otherwise inaccessible intermediates and transition states. On the other hand, the 1,2-dichloro-2-methylpropane reagent served as an oxidant. Note that one Ar-H is formed as side-product at each turnover during the manganese-mediated C-H activation step and that the final reductive elimination takes place in a pentacoordinated manganese(III) species.

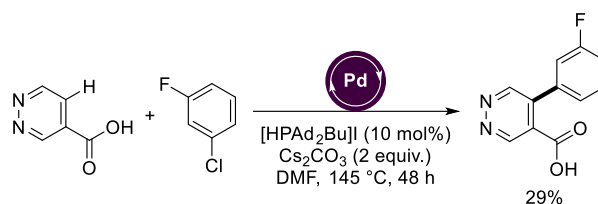


postulated mechanism



**Scheme 33** Intermolecular C-H *ortho*-arylation of pyrimidine by amide chelation under manganese catalysis (top) and plausible reaction mechanism (bottom). Mn =  $\text{MnCl}_2$  (10 mol%), S = THF solvent.

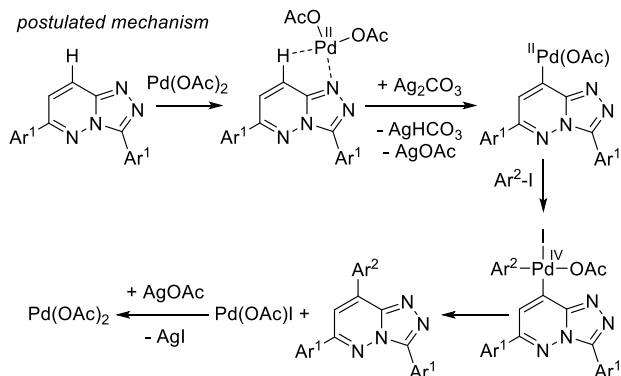
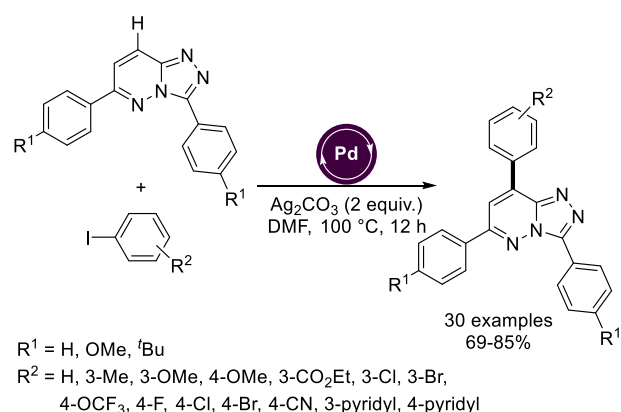
The Larrosa group developed palladium-catalyzed C-H arylation mediated by *ortho*-directing groups such as carboxylic acids.<sup>53</sup> In this context, they reported a single case of a pyridazine containing a carboxylic acid in C4 position that lead selectively to the C5 arylated derivative in 29% yield when using an aryl chloride coupling partner (Scheme 34). In addition, the authors demonstrated the relevance of generating the active species by *in situ* combination of  $\text{Pd}(\text{OAc})_2$  with a trialkylphosphane ligand.



**Scheme 34** Intermolecular C-H *ortho*-arylation of pyridazine by carboxylic acid chelation under palladium catalysis. Pd =  $\text{Pd}(\text{OAc})_2$  (5 mol%).



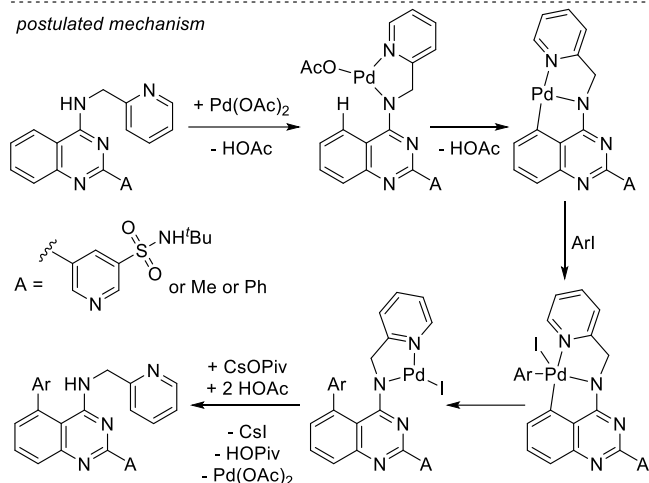
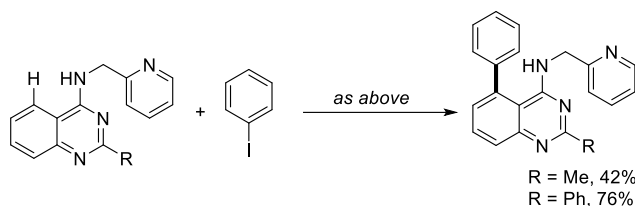
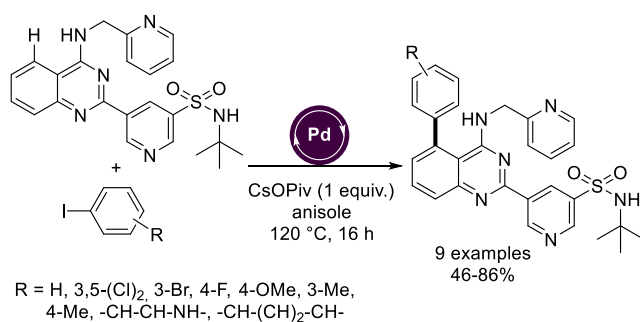
Maiti and co-workers developed selective C-H arylations in the pyridazine core under palladium catalysis.<sup>54</sup> By taking benefit from the directing ability of a rationally-placed 1,2,4-triazole motif nearby the C-H activation site, a large number of functional groups were tolerated including pyridine derivatives (Scheme 35, top). Importantly, the reaction conditions did not require the use of any phosphine ligand. The reactions lasted 12 hours with relatively high yields. The reaction mechanism is thought to begin with a C-H activation step mediated by palladium in the C-H from the diazine core neighbouring to the triazole ring (Scheme 35, bottom). After oxidative addition with the aryl iodide coupling partner and subsequent reductive elimination the final arylated diazine product is formed and Pd(OAc)I undergoes a final anion metathesis to regenerate the active Pd(OAc)<sub>2</sub> catalyst.



**Scheme 35** Intermolecular C-H arylation of pyridazine-based fused 1,2,4-triazoles under palladium catalysis (top) and plausible reaction mechanism (bottom). Pd = Pd(OAc)<sub>2</sub> (5 mol%).

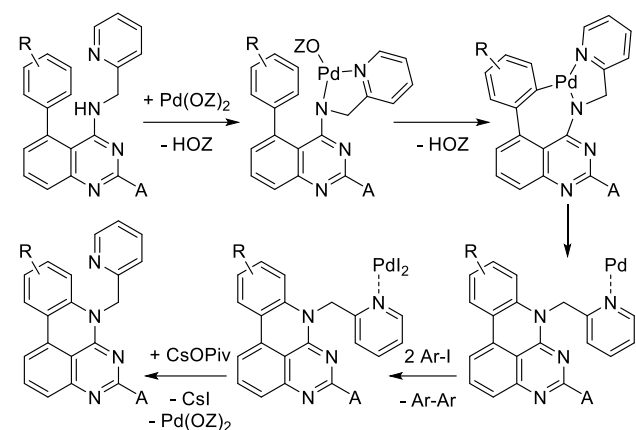
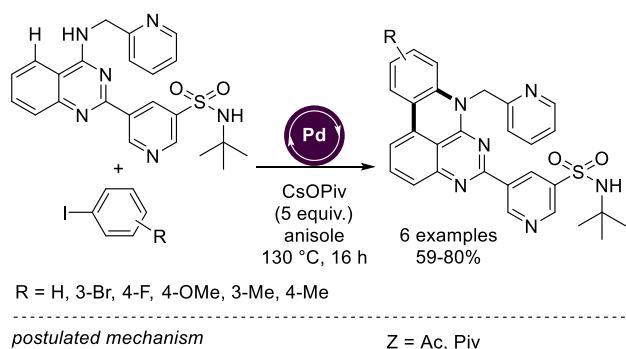
The Bristol-Myers Squibb Company developed palladium-catalyzed C-H arylations on a quinazoline derivative in order to access libraries structurally related to the I<sub>KuR</sub> inhibitor BMS-919373.<sup>55</sup> The key precursor contains a 2-picolylamine group that behaved as directing group in order to reach selective C5 arylation (Scheme 36, top). The catalysis performed well only with the more reactive (hetero)aryl iodides as coupling partners under phosphine-free palladium conditions with anisole as the solvent. Similar quinazoline derivatives afforded comparable levels of reactivity (Scheme 36, middle). The reaction mechanism for this palladium-catalyzed C-H arylation of diazine starts with the coordination of palladium to the *N,N*-chelating fragment in the substrate (Scheme 36, bottom). C-H activation at the C5 site leads to a *C,N,N*-pincer-like palladabicyclic species that follows oxidative addition with the aryl iodide and final reductive

eliminations towards the formation of the observed product and formation of the active Pd(OAc)<sub>2</sub> catalyst.



**Scheme 36** Intermolecular C-H bond (hetero)arylation of a biologically important quinazoline derivative under palladium catalysis (top), application to a less sophisticated system (middle) and plausible reaction mechanism (bottom). Pd = Pd(OAc)<sub>2</sub> (5 mol%).

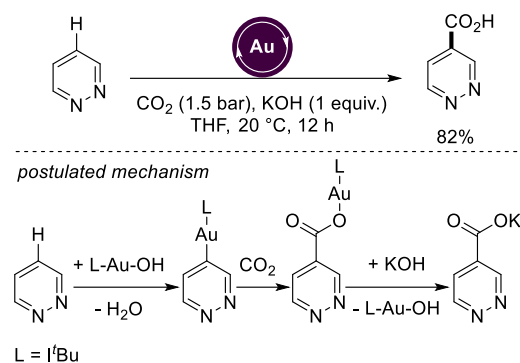
The same authors also noted that raising the number of equivalents of base to five as well as doubling the amounts of palladium precursor led an additional C-N bond forming reaction between the firstly introduced phenyl group and the amine group from the directing group (Scheme 37, top).<sup>56</sup> As such, original late-stage functionalization are targeted using palladium-catalyzed C-H arylation methodologies. Regarding the reaction mechanism (Scheme 37, bottom), once the C-H arylation takes place (Scheme 36), palladium coordinates to the *N,N*-chelating fragment within the substrate leading a *ortho*-C-H activation in the newly installed aryl motif followed by reductive carbon-nitrogen elimination. The remaining palladium species is re-oxidized by the excess aryl iodide as observed by the formation of biphenyl as side-product during the catalysis.



**Scheme 37** Inter- and intramolecular C-H functionalization of a biologically important quinazoline derivative under palladium catalysis (top) and plausible reaction mechanism (bottom). Pd = Pd(OAc)<sub>2</sub> (10 mol%).

## 6 Transition metal-catalyzed C-H carboxylation of diazines

In 2010, Nolan's group reported which is so far the only example of C-H carboxylation within the diazine core, namely pyridazine (Scheme 38, top).<sup>57</sup> The catalyst design is based on a gold-carbene complex that catalyzes the CO<sub>2</sub> insertion at the most acidic C-H bond leading to a useful heteroaromatic carboxylic acid scaffold in 82% yield. The protocol required one equivalent of KOH in the gold-catalyzed step and acidic treatment in a second step. This reaction aims at creating value from the greenhouse gas CO<sub>2</sub>. The reaction mechanism of this gold-catalyzed C-H functionalization of diazine is depicted in Scheme 38 (bottom). The gold-hydroxide carbene complex abstracts the hydrogen from the substrate with formation of water as side-product and formation of a new gold-carbon bond. CO<sub>2</sub> inserts in this bond carboxylate bound gold carbene species that undergoes ligand exchange with hydroxide forming back the active gold-carbene species and the carboxylated product that can be protonated during the work-up at the end of the reaction.



**Scheme 38** Gold-catalyzed C-H carboxylation of pyridazine with CO<sub>2</sub> under gold catalysis (top) and plausible reaction mechanism (bottom). Au = (<sup>t</sup>Bu)AuOH (1.5 mol%).

## 7 Conclusion

We have summarized the main discoveries concerning the selective C-H functionalization of diazines enabling formation of new C-C bond forming processes. In particular, C-H olefinations and C-H arylations appear to be the most reliable ones so far, although examples of alkylation, alkynylation and carboxylation are known. However, in general, the yields obtained from all the above-discussed metal-catalyzed methodologies are rather modest compared to the non-heteroaromatic versions. This clearly highlights the difficulty to directly perform C-H functionalizations on diazines. On the other hand, since diazine motifs are important building blocks in a variety of fields, it is of high interest and urgency to further develop technologies to circumvent the poor reactivity encountered not to mention to address selectivity issues when multiple C-H sites are available for reaction. Interestingly, as diazines are also well used as directing groups for C-H functionalizations,<sup>58-74</sup> examples merging this strategy with direct C-H functionalization at the diazine core in a one-pot or cascade manner might be appealing to undertake.<sup>75</sup> With this review, we hope to stimulate the scientific community on developing efficient tools to tackle C-H functionalizations of diazines en route to complex structures.

## Funding Information

Financial support from the Agence Nationale de la Recherche (ANR-19-CE07-0039), CNRS and University of Rennes 1 is acknowledged.

## Conflict of Interest

The authors declare no conflict of interest.

## References

- (a) Maes, B. U. W.; Lemière, G. L. F. In *Comprehensive Heterocyclic Chemistry III*; Katritzky, A. R.; Ramsden, C. A.; Scriven, E. F. V.; Taylor, R. J. K. (Eds.); Elsevier: Amsterdam, **2008**, Vol. 8, 1. (b) Rewcastle, G. W. In *Comprehensive Heterocyclic Chemistry III*; Katritzky, A. R.; Ramsden, C. A.; Scriven, E. F. V.; Taylor, R. J. K. (Eds.); Elsevier: Amsterdam, **2008**, vol. 8, 117. (c) Sato, N. In *Comprehensive Heterocyclic Chemistry III*; Katritzky, A. R.; Ramsden, C. A.; Scriven, E. F. V.; Taylor, R. J. K. (Eds.); Elsevier: Amsterdam, **2008**, vol. 8, 273. (d) Pozharskii, A. F.; Sodatenkov, A. T.; Katritzky, A. R. *Heterocycles in Life and Society: An Introduction to Heterocyclic Chemistry, Biochemistry and Applications, Second Edition*, Wiley: Chichester, **2011**. (e) Vitaku, E.; Smith, D. T.; Njardarson, J. T. *J. Med. Chem.* **2014**, *57*, 10257. (f) Baumann, M.; Baxendale, I. R. *Beilstein J. Org. Chem.*

- 2013, 9, 2265. (g) Yamaguchi, J.; Yamaguchi, A. D.; Itami, K. *Angew. Chem. Int. Ed.* **2012**, *51*, 8960. (h) Vila, N.; Besada, P.; Costas, T.; Costas-Lago, M. C.; Teran, C. *Eur. J. Med. Chem.* **2015**, *97*, 462. (i) Sergeev, P. V.; Nenajdenko, V. G. *Russ. Chem. Rev.* **2020**, *89*, 393.
- (2) (a) Itami, K.; Yamazaki, D.; Yoshida, J.-I. *J. Am. Chem. Soc.* **2004**, *126*, 15396. (b) Achelle, S.; Plé, N. *Curr. Org. Synth.* **2012**, *9*, 163. (c) Achelle, S.; Baudequin, C. In *Targets in Heterocyclic Systems*; Attanasi, O. A.; Spinelli D. (Eds.); Soc. Chim. Italiana: Roma, **2013**, vol. 17, 1. (d) Ortiz, R. P.; Casado, J.; Hernandez, V.; Lopez Navarrete, J. T.; Letizia, J. A.; Ratner, M. A.; Facchetti, A.; Marks, T. J. *Chem. Eur. J.* **2009**, *15*, 5023.
- (3) (a) Verbitskiy, E. V.; Rusinov, G. L.; Chupakhin, O. N.; Charushin, V. N. *Synthesis* **2018**, *50*, 193. (b) Charushin, V.N.; Chupakhin, O. N. *Pure Appl. Chem.* **2004**, *76*, 1621. (c) Chupakhin, O. N.; Charushin, V.N. *Tetrahedron Lett.* **2016**, *57*, 2665.
- (4) (a) Duncton, M. A. J. *MedChemComm* **2011**, *2*, 1135. (b) Proctor, R. S. J.; Phipps, R. J. *Angew. Chem. Int. Ed.* **2019**, *58*, 13666. (c) Yanagisawa, S.; Ueda, K.; Taniguchi, T.; Itami, K. *Org. Lett.* **2008**, *10*, 4673. (d) Thatikonda, T.; Singh, U.; Ambala, S.; Vishwakarma, R. A.; Singh, P. P. *Org. Biomol. Chem.* **2016**, *14*, 4312. (e) Ambala, S.; Thatikonda, T.; Sharma, S.; Munagala, G.; Yempalla, K. R.; Vishwakarma, R. A.; Singh, P. P. *Org. Biomol. Chem.* **2015**, *13*, 11341. (f) Seiple, I. B.; Su, S.; Rodriguez, R. A.; Gianatassio, R.; Fujiwara, Y.; Sobel, A. L.; Baran, P. S. *J. Am. Chem. Soc.* **2010**, *132*, 13194.
- (5) (a) Chevallier, F.; Mongin, F. *Chem. Soc. Rev.* **2008**, *3*, 595. (b) Seggio, A.; Chevallier, F.; Vaultier, M.; Mongin, F. *J. Org. Chem.* **2007**, *72*, 6602. (c) Balkenhohl, M.; Knochel, P. *SynOpen* **2018**, *2*, 78. (d) Groll, K.; Manolikakes, S. M.; du Jourdin, X. M.; Jaric, M.; Bredihhin, A.; Karaghiosoff, K.; Carell, T.; Knochel, P. *Angew. Chem. Int. Ed.* **2013**, *52*, 6776. (e) Rossi, R.; Lessi, M.; Manzini, C.; Marianetti, G.; Bellina, F. *Adv. Synth. Catal.* **2015**, *357*, 3777.
- (6) Selected representative examples: (a) Wimmer, L.; Rycek, L.; Koley, M.; Schnürch, M. *Top. Heterocyclic Chem.* **2014**, *45*, 61. (b) Maes, B. U. W.; Tapolcsanyi, P.; Meuers, C.; Matyus, M. *Curr. Org. Chem.* **2006**, *10*, 377. (c) Guram, A. S.; King, A. O.; Allen, J. G.; Wang, X.; Schenkel, L. B.; Chan, J.; Bunel, E. E.; Faul, M. M.; Larsen, R. D.; Martinelli, M. J.; Reider, P. J. *Org. Lett.* **2006**, *8*, 1787. (d) Lee, D.-H.; Jung, J.-Y.; Jin, M.-J. *Green Chem.* **2010**, *12*, 2024. (e) Stanetty, P.; Hattinger, G.; Schnürch, M.; Mihovilovic, M. D. *J. Org. Chem.* **2005**, *70*, 5215. (f) Beneritter, P.; de Araujo-Junior, J. X.; Schmitt, M.; Bourguignon, J.-J. *Tetrahedron* **2007**, *63*, 12465. (g) Fürstner, A.; Letner, A.; Mendez, M.; Krause, H. *J. Am. Chem. Soc.* **2002**, *124*, 13856.
- (7) (a) Gensch, T.; Hopkinson, M. N.; Glorius, F.; Wencel-Delord, J. *Chem. Soc. Rev.* **2016**, *45*, 2900. (b) Sambiagio, C.; Schönbauer, D.; Blicek, R.; Dao-Huy, T.; Pototschnig, G.; Schaaf, P.; Wiesinger, T.; Zia, M. F.; Wencel-Delord, J.; Besset, T.; Maes, B. U. W.; Schnürch, M. *Chem. Soc. Rev.* **2018**, *47*, 6603. (c) Hartwig, J. F.; Larsen, M. A. *ACS Cent. Sci.* **2016**, *2*, 281. (d) Rogge, T.; Kaplaneris, N.; Chatani, N.; Kim, J.; Chang, S.; Punji, B.; Schafer, L. L.; Musaev, D. G.; Wencel-Delord, J.; Roberts, C. A.; Sarpong, R.; Wilson, Z. E.; Brimble, M. A.; Johansson, M. J.; Ackermann, L. *Nat. Rev. Methods Primers*, **2021**, *1*, 43. (e) Gandeepan, P.; Müller, T.; Zell, D.; Cera, G.; Warratz, S.; Ackermann, Lutz, *Chem. Rev.* **2019**, *119*, 2192. (f) Gandeepan, P.; Finger, L. H.; Meyer, T. H.; Ackermann, L. *Chem. Soc. Rev.* **2020**, *49*, 4254. (g) Loup, J.; Dhawa, U.; Pesciaoli, F.; Wencel-Delord, J.; Ackermann, L. *Angew. Chem. Int. Ed.* **2019**, *58*, 12803. (h) Rossi, R.; Lessi, M.; Manzini, C.; Marianetti, G.; Bellina, F. *Tetrahedron* **2016**, *72*, 1795. (i) Théveau, L.; Schneider, C.; Fruit, C.; Hoarau, C. *ChemCatChem* **2016**, *8*, 3183. (j) Rossi, R.; Ciofalo, M. *Curr. Org. Chem.* **2022**, *26*, 215. (k) Murakami, K.; Yamada, S.; Kaneda, T.; Itami, K. *Chem. Rev.* **2017**, *117*, 9302.
- (8) Tran, G.; Hesp, K. D.; Mascitti, V.; Ellman, J. A. *Angew. Chem. Int. Ed.* **2017**, *56*, 5899.
- (9) (a) Wiedemann, S. H.; Ellman, J. A.; Bergman, R. G. *J. Org. Chem.* **2006**, *71*, 1969. (b) Wiedemann, S. H.; Lewis, J. C.; Ellman, J. A.; Bergman, R. G. *J. Am. Chem. Soc.* **2008**, *128*, 2452.
- (10) Gribble Jr., M. W.; Guo, S.; Buchwald, S. L. J. *J. Am. Chem. Soc.* **2018**, *140*, 5057.
- (11) (a) Catellani, M.; Frignani, F.; Rangoni, A. *Angew. Chem. Int. Ed.* **1997**, *36*, 119. (b) Wang, J.; Dong, G. *Chem. Rev.* **2019**, *119*, 7478. (c) Lautens, M.; Piguél, S. *Angew. Chem. Int. Ed.* **2000**, *39*, 1045.
- (12) (a) Gao, Q.; Shang, Y.; Song, F.; Ye, J.; Liu, Z.-S.; Li, L.; Cheng, H.-G.; Zhou, Q. *J. Am. Chem. Soc.* **2019**, *141*, 15986.
- (13) Dong, Z.; Lu, G.; Wang, J.; Liu, P.; Dong, G. *J. Am. Chem. Soc.* **2018**, *140*, 8551.
- (14) Wang, X.; Zhao, S.; Liu, J.; Zhu, D.; Guo, M.; Tang, X.; Wang, G. *Org. Lett.* **2017**, *19*, 4187.
- (15) Zhang, S.; Weniger, F.; Kreyenschulte, C. R.; Lund, H.; Bartling, S.; Neumann, H.; Ellinger, S.; Taeschler, C.; Beller, M. *Catal. Sci. Technol.* **2020**, *10*, 1731.
- (16) Yi, J.; Yang, L.; Xia, C.; Li, F. *J. Org. Chem.* **2015**, *80*, 6213.
- (17) Liu, Y.-J.; Liu, Y.-H.; Yin, X.-S.; Gu, W.-J.; Shi, B.-F. *Chem. Eur. J.* **2015**, *21*, 205.
- (18) Ye, M.; Gao, G.-L.; Yu, J.-Q. *J. Am. Chem. Soc.* **2011**, *133*, 6964.
- (19) Cong, X.; Tang, H.; Wu, C.; Zeng, X. *Organometallics* **2013**, *32*, 6565.
- (20) Das, A.; Jana, A.; Maji, B. *Chem. Commun.* **2020**, *56*, 4284.
- (21) Wen, P.; Li, Y.; Zhou, K.; Ma, C.; Lan, X.; Ma, C.; Huang, G. *Adv. Synth. Catal.* **2012**, *354*, 2135.
- (22) Zhang, Z.; Tanaka, K.; Yu, J.-Q. *Nature* **2017**, *543*, 538.
- (23) Yin, B.; Fu, M.; Wang, L.; Liu, J.; Zhu, Q. *Chem. Commun.* **2020**, *56*, 3293.
- (24) Zhang, Z.; Zheng, Y.; Sun, Z.; Dai, Z.; Tang, Z.; Ma, J.; Ma, C. *Adv. Synth. Catal.* **2017**, *359*, 2259.
- (25) Zhou, J.; Li, B.; Qian, Z.-C.; Shi, B.-F. *Adv. Synth. Catal.* **2014**, *356*, 1038.
- (26) Cai, S.; Chen, C.; Shao, P.; Xi, C. *Org. Lett.* **2014**, *16*, 3142.
- (27) Nakao, Y.; Kanyiva, K. S.; Hiayama, T. *J. Am. Chem. Soc.* **2008**, *130*, 2448.
- (28) Wang, C.-S.; Di Monaco, S.; Thai, A. N.; Rahman, Md. S.; Pang, B. P.; Wang, C.; Yoshikai, N. *J. Am. Chem. Soc.* **2020**, *142*, 12878.
- (29) Morioka, R.; Nobushige, K.; Satoh, T.; Hirano, K.; Miura, M. *Org. Lett.* **2015**, *17*, 3130.
- (30) Karak, P.; Dutta, C.; Dutta, T.; Koner, A. L.; Choudhury, J. *Chem. Commun.* **2019**, *55*, 6791.
- (31) Meesa, S. R.; Naikawadi, P. K.; Gugulothu, K.; Kumar, K. S. *Org. Biomol. Chem.* **2020**, *18*, 3032.
- (32) Yang, Y.; Lan, J.; You, J. *Chem. Rev.* **2017**, *117*, 8787.
- (33) Liu, B.; Huang, Y.; Lan, J.; Song, F.; You, J. *Chem. Sci.* **2013**, *4*, 2163.
- (34) Ren, X.; Wen, P.; Shi, X.; Wang, Y.; Li, J.; Yang, S.; Yan, H.; Huang, G. *Org. Lett.* **2013**, *15*, 5194.
- (35) Yamada, S.; Kaneda, T.; Steib, P.; Murakami, K.; Itami, K. *Angew. Chem. Int. Ed.* **2019**, *58*, 8341.
- (36) Chen, C.; Chen, X.; Zhao, H.; Jiang, H.; Zhang, M. *Org. Lett.* **2017**, *19*, 3390.
- (37) (a) Campeau, L.-C.; Fagnou, K. *Chem. Commun.* **2006**, 1253. (b) Alberico, D.; Scott, M. E.; Lautens, M. *Chem. Rev.* **2007**, *107*, 174. (c) Seregin, I. V.; Gevorgyan, V. *Chem. Soc. Rev.* **2007**, *36*, 1173. (d) Ackermann, L. *Synlett* **2007**, 507. (e) Lewis, J. C.; Bergman, R. G.; Ellman, J. A. *Acc. Chem. Res.* **2008**, *41*, 1013. (f) Arockiam, P. B.; Bruneau, C.; Dixneuf, P. H. *Chem. Rev.* **2012**, *112*, 5879. (g) Hussain, I.; Singh, T. *Adv. Synth. Catal.* **2014**, *356*, 1661.
- (38) Do, H.-Q.; Khan, R. M. K.; Daugulis, O. *J. Am. Chem. Soc.* **2008**, *130*, 15185.
- (39) Do, H.-Q.; Daugulis, O. *J. Am. Chem. Soc.* **2009**, *131*, 17052.
- (40) Truong, T.; Alvarado, J.; Tran, L. D.; Daugulis, O. *Org. Lett.* **2010**, *12*, 1200.
- (41) (a) Tobisu, M.; Hyodo, I.; Chatani, N. *J. Am. Chem. Soc.* **2009**, *131*, 12070. (b) Hyodo, I.; Tobisu, M.; Chatani, N. *Chem. Asian J.* **2012**, *7*, 1357.
- (42) (a) Berman, A. M.; Bergman, R. G.; Ellman, J. A. *J. Org. Chem.* **2010**, *75*, 7863. (b) Lewis, J. C.; Wiedemann, S. H.; Bergman, R. G.; Ellman, J. A. *Org. Lett.* **2004**, *6*, 35. (c) Lewis, J. C.; Wu, J. Y.; Bergman, R. G.; Ellman, J. A. *Angew. Chem. Int. Ed.* **2006**, *45*, 1589.
- (43) Kwak, J.; Kim, M.; Chang, S. *J. Am. Chem. Soc.* **2011**, *133*, 3780.
- (44) Guchhait, S. K.; Kandekar, S.; Kashyap, M.; Taxak, N.; Bharatam, P. V. *J. Org. Chem.* **2012**, *77*, 8321.

- (45) Nguyen, Q.-H.; Guo, S.-M.; Royal, T.; Baudoin, O.; Cramer, N. *J. Am. Chem. Soc.* **2020**, *142*, 2161.
- (46) Zhang, J.; Parker, T. C.; Chen, W.; Williams, L.; Khrustalev, V. N.; Jucov, E. V.; Barlow, S.; Timofeeva, T. V.; Marder, S. R. *J. Org. Chem.* **2016**, *81*, 360.
- (47) Wei, D.; Li, M.-Y.; Zhu, B.-B.; Yang, X.-D.; Fang, Z.; Feng, C.-G.; Lin, G.-Q. *Angew. Chem. Int. Ed.* **2019**, *58*, 16543.
- (48) Shi, H.; Lu, Y.; Weng, J.; Bay, K. L.; Chen, X.; Tanaka, K.; Verma, P.; Houk, K. N.; Yu, J.-Q. *Nature Chem.* **2020**, *12*, 399.
- (49) Basolo, L.; Beccalli, E. M.; Borsini, E.; Broggini, G. *Tetrahedron* **2009**, *65*, 3486.
- (50) Zhao, Y.; Snieckus, V. *Adv. Synth. Catal.* **2014**, *356*, 1527.
- (51) Sirois, J.J.; Davis, R.; DeBoef, B. *Org. Lett.* **2014**, *16*, 868.
- (52) Zhu, C.; Oliveira, J. C. A.; Shen, Z.; Huang, H.; Ackermann, L. *ACS Catal.* **2018**, *8*, 4402.
- (53) Johnston, A. J. S.; Ling, K. B.; Sale, D.; Lebrasseur, N.; Larrosa, I. *Org. Lett.* **2016**, *18*, 6094.
- (54) Srinivasan, R.; Dey, A.; Nagarajan, N. S.; Kumaran, R. S.; Gandhi, T.; Maiti, *Chem. Commun.* **2017**, *53*, 11709.
- (55) Wisniewski, S. R.; Stevens, J. M.; Yu, M.; *J. Org. Chem.* **2019**, *84*, 4704.
- (56) Wisniewski, S. R.; Savage, S. A.; Romero, E. O.; *J. Org. Chem.* **2019**, *84*, 7961.
- (57) Boogaerts, I. I. F.; Nolan, S. P. *J. Am. Chem. Soc.* **2010**, *132*, 8858.
- (58) Gramage-Doria, R.; Achelle, S.; Bruneau, C.; Robin-le Guen, F.; Dorcet, V.; Roisnel, T. *J. Org. Chem.* **2018**, *83*, 1462.
- (59) Stefane, B.; Brodnik Zugelj, H. B.; Groselj, U.; Kuzman, P.; Svete, J.; Pozgan, F. *Eur. J. Org. Chem.* **2017**, 1855.
- (60) Kuzman, P.; Pozgan, F.; Meden, A.; Svete, J.; Stefane, B. *ChemCatChem* **2017**, *9*, 3380.
- (61) Hrovat, S.; Drev, M.; Grošelj, U.; Perdih, F.; Svete, J.; Štefane, B.; Požgan, F. *Catalysts* **2020**, *10*, 421.
- (62) Drev, M.; Grošelj, U.; Ledinek, B.; Perdih, F.; Svete, J.; Štefane, B.; Požgan, F. *ChemCatChem* **2018**, *10*, 3824.
- (63) Štefane, B.; Fabris, J.; Požgan, F.; *Eur. J. Org. Chem.* **2011**, 3474.
- (64) Benzai, A.; Derridj, F.; Doucet, H.; Soulé, J.-F. *ChemCatChem* **2021**, *13*, 338.
- (65) Idris, I.; Derridj, F.; Roisnel, T.; Doucet, H.; Soulé, J.-F. *New J. Chem.* **2018**, *42*, 16036.
- (66) Lakshman, M. K.; Deb, A. C.; Chamala, R. R.; Pradhan, P.; Pratap, R. *Angew. Chem. Int. Ed.* **2011**, *50*, 11400.
- (67) Guo, H.-M.; Jiang, L.-L.; Niu, H.-Y.; Rao, W.-H.; Liang, L.; Mao, R.-Z.; Li, D.-Y.; Qu, G.-R. *Org. Lett.* **2011**, *13*, 2008.
- (68) Wang, L.; Xiong, D.; Jie, L.; Yu, C.; Cui, X. *Chin. Chem. Lett.* **2018**, *29*, 907.
- (69) Leitch, J. A.; Heron, C. J.; McKnight, J.; Kociok-Köhn, G.; Bhonoahd, Y.; Frost, C. G. *Chem. Commun.* **2017**, *53*, 13039.
- (70) Bag, S.; Jayarajan, R.; Mondal, R.; Maiti, D. *Angew. Chem. Int. Ed.* **2017**, *56*, 3182.
- (71) Jayarajan, R.; Das, J.; Bag, S.; Chowdhury, R.; Maiti, D. *Angew. Chem. Int. Ed.* **2018**, *57*, 7659.
- (72) Achar, T. K.; Zhang, X.; Mondal, R.; Shanavas, M. S.; Maiti, S.; Maity, S.; Pal, N.; Paton, R. S.; Maiti, D. *Angew. Chem. Int. Ed.* **2019**, *58*, 10353.
- (73) Bag, S.; K. S.; Mondal, A.; Jayarajan, R.; Dutta, U.; Porey, S.; Sunoj, R. B.; Maiti, D. *J. Am. Chem. Soc.* **2020**, *142*, 12453.
- (74) Brochetta, M.; Borsari, T.; Bag, S.; Jana, S.; Maiti, S.; Porta, A.; Werz, D. B.; Zanon, G.; Maiti, D. *Chem. Eur. J.* **2019**, *25*, 10323.
- (75) Gramage-Doria, R.; Bruneau, C. *Coord. Chem. Rev.* **2021**, *428*, 21362.